Revue de micropaléontologie 87 (2025) 100841

Contents lists available at ScienceDirect

Revue de micropaléontologie

journal homepage: www.elsevier.com/locate/revmic

Research paper

Paleoecology of Early Ladinian low-diversity radiolarian fauna from Mt. Svilaja (External Dinarides, Croatia)

Špela Goričan[a,*], Tea Kolar-Jurkovšek[b], Dunja Aljinović[c], Tamara Troskot-Čorbić[d], Bogdan Jurkovšek[e]

[a] ZRC SAZU, Ivan Rakovec Institute of Palaeontology, SI-1000 Ljubljana, Slovenia
[b] Geological Survey of Slovenia, SI-1000 Ljubljana, Slovenia
[c] University of Zagreb, Faculty of Mining, Geology and Petroleum Engineering, HR-10000 Zagreb, Croatia
[d] INA-Industrija nafte d.d., HR-10000 Zagreb, Croatia
[e] Kamnica 27, 1262 Dol pri Ljubljani, Slovenia

ARTICLE INFO

Keywords:
Radiolaria
Conodonts
Middle Triassic
Anoxic intra-platform basin
Dinarides

ABSTRACT

Dark-grey cherty limestone from Mt. Svilaja contains moderately well-preserved radiolarians of unusually low diversity. Nineteen genera were encountered, namely, only one fourth of genera known from the time equivalent Buchenstein Formation. Based on conodonts, the studied interval is assigned to the Lower Ladinian *Budurovignathus hungaricus* Zone. Ammonoids and allochthonous fossil elements (calcareous algae, corals, brachiopods, bivalves, benthic foraminifera, terrestrial-plant remains) from the same interval were previously reported. Facies and organic-matter analyses support the interpretation of depositional setting in a semi-enclosed basin with oxygen-deficient bottom waters. The radiolarian assemblage consists of spherical Entactinaria (Pentactinocarpidae, Heptacladidae, Hindeosphaeridae) and Spumellaria (*Archaeocenosphaera, Paurinella, Triassospongosphaera, Spongopallium*), and monocyrtid Nassellaria (mostly *Hozmadia*). Among Pentactinocarpidae, *Lobactinocapsa ellipsoconcha* Dumitrica is abundant and characterized by considerable variability of the cortical shell regarding its shape (ovoid to spherical), wall thickness (single-layered to spongy), and number of external spines. Eptingiidae, Oertlispongidae, Relindellidae, and all multicyrtid Nassellaria, common in the Buchenstein Formation as well as in radiolarian cherts associated with ophiolites, are missing. Similar, although less drastically reduced radiolarian fauna is known from the coeval San Giorgio Dolomite, which was also deposited in an oxygen-deficient intra-platform basin. The San Giorgio fauna lacks multicyrtid Nassellaria but still contains abundant Eptingiidae, Oertlispongidae, and Relindellidae. The likely factor reducing the diversity in the intra-platform basins was the vertical extent of the oxygen-deficient lower water column. Only surface-dwelling radiolarians were successful in stratified basins with expanded deep-water hypoxia.

1. Introduction

Low latitude Late Anisian and Early Ladinian radiolarians have been extensively studied worldwide and are well known from open-marine facies of continental margins, e.g., the Buchenstein and equivalent formations in the Mediterranean region (Dumitrica, 1978a, 1978b; 1982a, 1982b; Dumitrica et al., 1980; Kozur and Mostler, 1981, 1994; Kolar-Jurkovšek, 1989; Goričan and Buser, 1990 etc.), as well as the oceanic bedded cherts of Japan (Sugiyama, 1997), Philippines (Cheng, 1989; Yeh, 1990), Indonesia (Sashida et al., 1999), Thailand (Sashida et al., 2000) and the Himalayas (Chen et al., 2019). When well preserved, these radiolarian assemblages are very diverse. Up to 170 species pertaining to 71 genera have been found in a single sample of the Buchenstein Formation (Ozsvárt et al., 2023). In contrast, coeval radiolarian assemblages of intra-platform basins seem to be considerably reduced in diversity but their record is scarce. Just one example from the San Giorgio Dolomite in the Southern Alps (Stockar et al., 2012) has thus far been published.

The studied section from Mt. Svilaja (External Dinarides, Croatia) is characterized by dark-grey carbonates with intercalations of pyroclastic rocks (Pietra Verde). The locality is long known for well-preserved fossils of various groups: terrestrial plants (Kerner, 1907), algae, calcareous sponges, corals, crinoids, brachiopods, gastropods, bivalves and, in thin sections, also benthic foraminifera, radiolarians and possibly conodonts (Chorowicz and Termier, 1975). Based on the presence of organic matter and pelagic fauna, the depositional environment is interpreted as a

* Corresponding author.
E-mail address: spela.gorican@zrc-sazu.si (Š. Goričan).

https://doi.org/10.1016/j.revmic.2025.100841

semi-enclosed oxygen-depleted basin (intra-shelf anoxic depression in Belak, 2000). Calcareous benthos and terrestrial plants originated from adjacent shallow-water and land areas. Several recent papers focused on individual fossil groups from this locality. Conodont stratigraphy was established by Jelaska et al. (2003), ammonoids were studied by Balini et al. (2006) and brachiopods by Halamski et al. (2015), but radiolarians have not been investigated in detail yet. They are particularly abundant in one stratigraphic level. The radiolarian assemblage is characterized by the extremely low diversity and high relative abundance of spheroidal forms with a spongy cortical shell. The entire deep-water succession is dated with conodonts from the *constricta* Zone (Illyrian) to the *murcianus* Zone (?uppermost Longobardian–lower Julian); the radiolarian-bearing limestone is assigned to the *hungaricus* conodont Zone (Fassanian) (Jelaska et al., 2003 and new results in this study).

The aim of this paper is to present a complete inventory of this peculiar Early Ladinian radiolarian assemblage. Conodonts were re-studied with higher-resolution sampling than previously to produce a solid time framework for the radiolarian-bearing interval. Facies analysis along with microscopic and geochemical studies of organic matter were performed to obtain specific data on the depositional environment. Comparisons with coeval higher-diversity radiolarian assemblages from more open-marine settings are discussed and a circulation model to explain the low-diversity is proposed. The results contribute to the understanding of the paleoecology of Middle Triassic radiolarians and may also be useful for explaining the impoverished radiolarian assemblages of other ages.

2. Geological setting

2.1. Regional geology

The Svilaja Mountain to the north of Split in central Dalmatia is part of the High Karst Zone in the External Dinarides (Fig. 1). In the Mesozoic, the area pertained to the proximal continental margin of the Adria microplate, which was bounded to the east by the Meliata-Maliac branch of the Neotethys. Continuous sea-floor spreading from the Late Anisian to the Norian has been documented along nearly the entire length of this oceanic branch, i.e., from southern Slovakia and Hungary through Croatia, Serbia, Albania, and Greece (e.g., Goričan et al., 2005; Chiari et al., 2012; Ozsvárt and Kovács, 2012; Ferrière et al., 2015, 2016, with references; Gawlick et al., 2016; Kukoč et al., 2024).

The continental break-up was preceded by rifting, which started in the Middle Anisian and resulted in the complex horst-and-graben paleotopography of the Adriatic continental margin. The differential subsidence and drowning of formerly uniform Early–Middle Anisian carbonate platforms have been well documented in the Southern Alps (e.g., Bechstädt et al., 1978; Gianolla et al., 1998 and the references therein; Berra and Carminati, 2010; Preto et al., 2011) including the area of overlap with the Dinarides (Celarc et al., 2013 with references), and also in the Eastern Alps (Gawlick et al., 2021 with references) and the Pelso Unit in Hungary (Budai and Vöros, 1993; Haas and Budai, 1999; Velledits, 2006).

In the Dinarides, the rifting processes, associated volcanism, and horst-and-graben topography of the margin were already documented in regional studies in the 1970s (Rampnoux, 1974; Chorowicz, 1977; Cadet, 1978; Charvet, 1978). The most deeply subsided basins (e.g., the Budva, Bosnian, and Slovenian basins) remained sites of pelagic sedimentation until the latest Cretaceous. Shallower basins formed on structural highs, which were internally differentiated into several fault blocks. These shallow basins were short lived, limited to the interval between the Middle–Late Anisian to Ladinian or Early Carnian, when they were completely filled in such that the sedimentation of platform carbonates was again established in a wider area. Recent papers focused on syn- and early post-rift deposits of these shallower basins provided extremely precise biostratigraphic data (e.g., Sudar et al., 2013, 2023; Kolar-Jurkovšek et al., 2023; Mrdak et al., 2024) and locally very detailed reconstructions of the continental margin (e.g., Kukoč et al., 2023).

The High Karst Zone consists of a several-thousand-meter-thick series of Triassic to Upper Cretaceous platform carbonates and, in the Triassic, was the largest structural high on the eastern continental margin of Adria. The zone now extends from Slovenia and north-eastern Italy to the Skutari–Peć transverse line in northern Albania (Fig. 1). In terms of paleogeography, this large carbonate platform is known as the High Karst or Dinaric (in Italian literature also Friuli) Carbonate Platform. According to Vlahović et al. (2005), it belongs to the vast Southern Tethyan Megaplatform in the Middle to Late Triassic and forms the NE part of the future (post-Early Toarcian) Adriatic Carbonate Platform.

Two types of sequences from the short Middle Triassic pelagic episode are preserved in the High Karst Zone. Both are characterized by micritic limestone and chert, generally include pyroclastic rocks (Pietra Verde), and locally contain carbonate breccia and calcarenite. The most obvious difference is the color of the rocks. The successions in the center of the High Karst Zone, like that of Mt. Svilaja in this study, are dark-grey to black and often dolomitic. Such dark carbonate facies occur from northern Dalmatia (e.g., Smirčić et al., 2018, 2020) to the Albanian Alps (the Theth Formation formally described by Gaetani et al., 2015). In contrast, the pelagic limestone and chert at the margins of the High Karst swell are light to vivid-red, in places greenish or light-grey to pink. This latter lithology is comparable with the Buchenstein Formation of the Southern Alps and is known from the NE margin of the High Karst swell facing the Bosnian Basin (e.g., Mudrenović and Gaković, 1964) as well as its SW margin adjacent to the Budva Basin (Gawlick et al., 2012).

2.2. Stratigraphy of Mt. Svilaja

The succession in the study area (Fig. 2) starts with 350 m of Lower Triassic shelf siliciclastics and carbonates, classically known from the Southern Alps as the Seis and Campil beds. These Lower Triassic beds are unconformably overlain by the dolomitic Anisian Otarnik breccia and then by an approximately 150-m-thick succession of dark-grey pelagic carbonates and pyroclastic rocks (Pietra Verde). The main Pietra Verde horizon is a 10-m-thick unit of crystaloclastic and vitriclastic tuff with elevated SiO_2 content (75%), probably related to additional silicification during diagenesis (Šćavničar et al., 1984; Smirčić et al., 2018). The entire section has been dated with conodonts (Jelaska et al., 2003; see Fig. 2 for the position of conodont zones). The *Pachycladina obliqua* conodont zone (Smithian) was determined near the base of the section and five consecutive conodont zones were distinguished in the pelagic interval. These zones are the *Neogondolella constricta* Zone (Illyrian) just above the Otarnik breccia, the *Paragondolella trammeri* Zone (Illyrian–Fassanian), *Budurovignathus hungaricus* Zone (Fassanian), *Budurovignathus mungoensis* Zone (Longobardian), and the *Pseudofurnishius murcianus* Zone (?uppermost Longobardian–lower Julian). The deeper water carbonates are overlain by an emersion breccia with bauxitic clayey matrix that is followed by thick-bedded Norian-Rhaetian limestone and dolomite (Bucković and Martinuš, 2010).

The carbonates above the main Pietra Verde horizon are known for numerous well-preserved usually silicified fossil remains, such as dasycladalean algae, benthic foraminifera, crinoids, calcisponges, corals, brachiopods, gastropods and bivalves (Chorowicz and Termier, 1975). In the bituminous carbonates, plant debris (pteridosperms and probably conifers) were found (Kerner, 1907). Since the beds with the most prolific and diverse biota were precisely dated to the *hungaricus* conodont Zone (Jelaska et al., 2003; Kolar-Jurkovšek et al., 2006), several groups have been studied in detail. Calcareous algae are abundant, with the most common species among them being *Diplopora annulata* Schafhäutl and *Teutloporella herculea* (Stoppani) Pia (Grgasović et al., 2007). Ammonoid fauna is composed of both leiostraca (*Proarcestes* sp.) and trachyostraca, the latter with three species first described from this section (*Alkaites dinaricus* Balini, Jurkovšek, and Kolar-Jurkovšek, *Detoniceras svilajanus* Balini, Jurkovšek, and Kolar-Jurkovšek, and *Ar-*

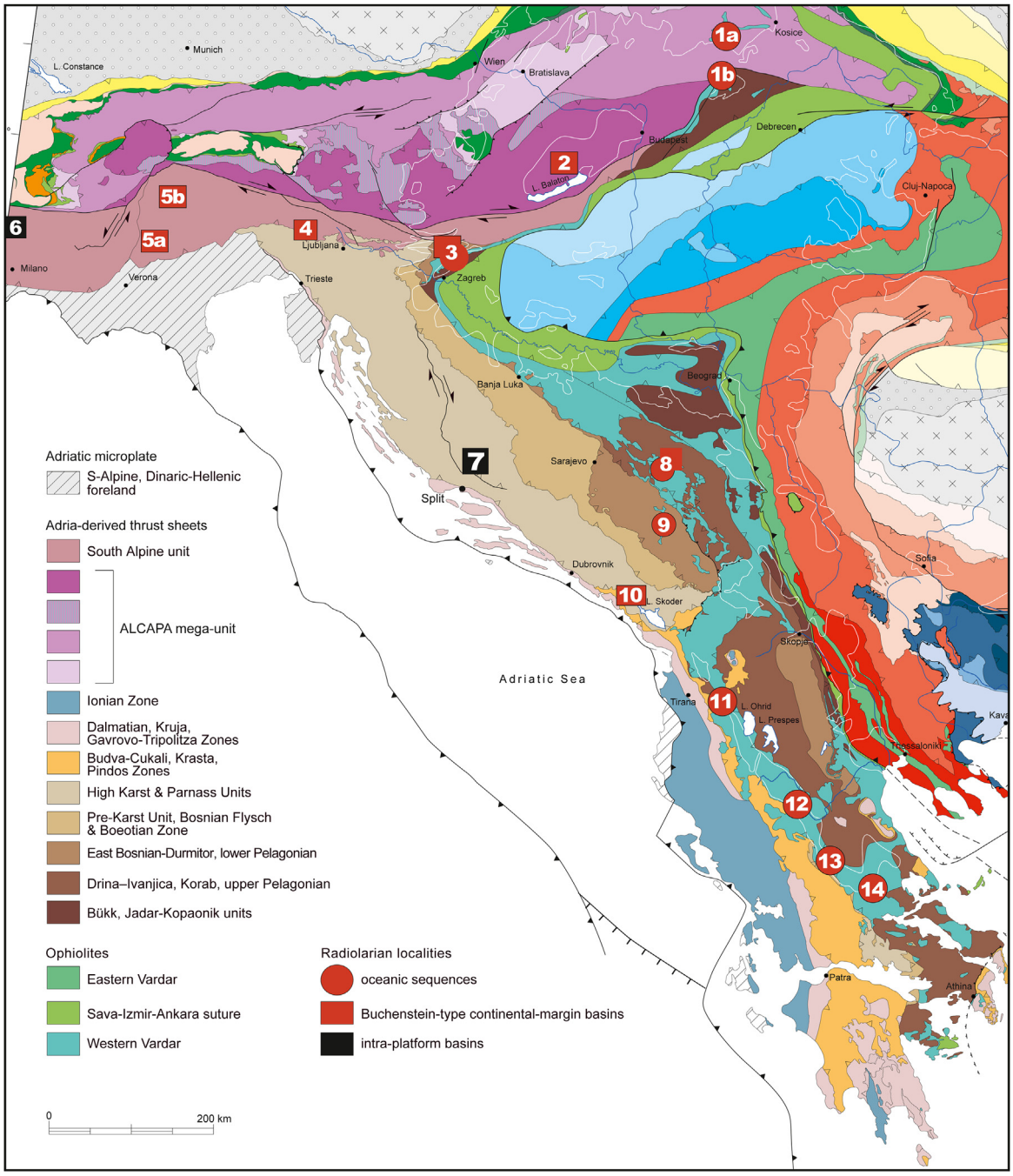

Fig. 1. Location map showing the Svilaja section (no. 7) and other localities with radiolarian assemblages of *Spongosilicarmiger italicus* and/or *Ladinocampe multiperforata* zones (uppermost Anisian–Lower Ladinian). Tectonic map according to Schmid et al. (2020) (polygons courtesy of S.M. Schmid). The symbols for localities denote their paleogeographic setting: red circles = oceanic sequences; red squares = Buchenstein-type continental-margin basins; black squares = intra-platform basins.

(1a, b) SE Slovakia and NE Hungary (Meliata and Darnó units) – Dumitrica and Mello (1982), Kozur and Réti (1986), Dosztály and Józsa (1992). (2) Balaton Highland – Kozur and Mostler (1981, 1994). (3) N Croatia (Medvednica, Kalnik, Ivanščica) – Goričan et al. (2005), Slovenec et al. (2020), Kukoč et al. (2023, 2024). (4) W Slovenia (Julian Alps and External Dinarides) – Goričan and Buser (1990). (5a, b) Buchenstein-type basins of the Southern Alps (Vicentinian Prealps, Dolomites) – Dumitrica (1978a, 1978b,1982a, 1982b), Dumitrica et al. (1980), Kozur and Mostler (1981, 1994), Lahm (1984), Kellici and De Wever (1995), Ozsvárt et al. (2023). (6) Monte San Giorgio – Stockar et al. (2012). (7) Mt. Svilaja – this study. (8) W Serbia (Ovčar Banja) – Obradović and Goričan (1988), Vishnevskaya et al. (2009), Djerić et al. (2024). (9) NE Montenegro (Drno Brdo) – Goričan et al. (2022). (10) SW Montenegro, High Karst Zone – Gawlick et al. (2012). (11) Albania (Mirdita Ophiolite Zone) – Marcucci et al. (1994), Chiari et al. (1996), Gawlick et al. (2008, 2016). (12) Pindos ophiolite – Ozsvárt et al. (2012). (13) Koziakas – Chiari et al. (2012). (14) Othris – Ferrière et al. (2015).

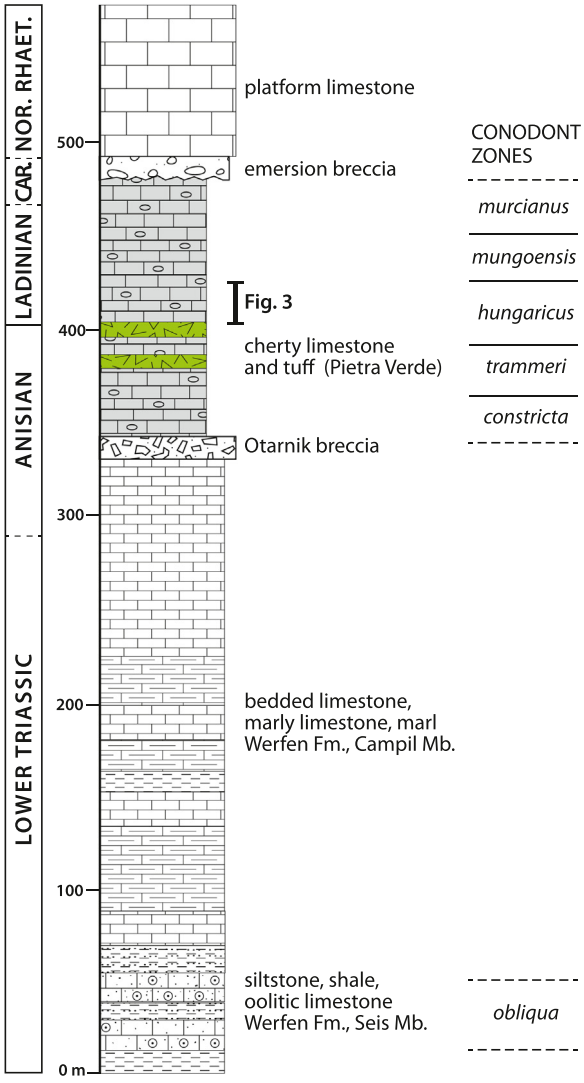

Fig. 2. Synthetic stratigraphic log and conodont dating of the Lower to Upper Triassic succession at Mt. Svilaja (according to Jelaska et al., 2003). The black bar in the *Budurovignathus hungaricus* Zone indicates the position of the section presented in Fig. 3.

golites trinodosus Balini, Jurkovšek, and Kolar-Jurkovšek) (Balini et al., 2006). These strata also yield abundant albeit low diversity brachiopod fauna, which consists of five species (Halamski et al., 2015). The most common and predominating is *Flabellocyrtia flabellulum* Chorowicz and Termier (1975), previously described from the same locality. The accompanying species are *Cassianospira humboldtii* (von Klipstein), which is the only species known elsewhere, two newly described species *Thecocyrtella dagysii* Halamski et al. (2015) and *Albasphe albertimagni* Halamski et al. (2015), and a poorly preserved Terebratulidina? gen. et sp. indet. This brachiopod assemblage is interpreted as parautochthonous and representing the ecosystem of a dasycladalean submarine meadow (Halamski et al., 2015). Significantly, the ammonoid and brachiopod faunas are characterized by pronounced endemism.

3. Material and methods

A small portion of the section above the main Pietra Verde horizon was investigated in greater detail to provide a solid environmental and temporal framework for the peculiar radiolarian faunas in this interval. Conodonts were studied to refine the previously established stratigraphy and these data were complemented with sedimentological and organic-matter analyses to allow for a better characterization of the basin. Field work including measuring and sampling was performed in 2015. The measured section (Fig. 3) is located close to the village of Zelovo about 5 km NW from Sinj (location coordinates N 43° 42′ 49″, E 16° 32′ 05″; for access, see fig. 1 in Jelaska et al., 2003).

Nine samples were collected for conodonts with a minimum weight of 2 kg each and were processed for conodont study using standard laboratory techniques with acetic acid dissolution (ca. 7%–10%). The residues of all samples contained determinable conodonts and in two of them radiolarians were also found. Processing was conducted at the Geological Survey of Slovenia / Geološki zavod Slovenije in Ljubljana. The conodont material is stored, inventoried, and abbreviated as GeoZS under repository numbers 5758–5766 in the micropaleontological collection of the Geological Survey of Slovenia where photographs of the conodont elements presented in this paper were taken (JEOL JSM 6490LV Scanning Electron Microscope). Radiolarians were photographed at ZRC SAZU with JEOL JSM IT100 and are stored in the collection of the Ivan Rakovec Institute of Palaeontology ZRC SAZU.

The thin sections for determining petrographic features underwent a standard staining procedure utilizing K-ferricyanide and Alizarin Red S (Dickson, 1965) and were studied with the use of plane polarizing light microscopy at the University of Zagreb, Faculty of Mining, Geology and Petroleum Engineering, with an Optika B-1000 Pol polarizing microscope, and a CPL-6 Optika camera operated with ProView software.

Organic geochemistry was conducted to determine the quantity, quality, and maturity of organic matter. The total organic carbon (TOC) content of 19 samples, expressed as wt. %, was performed on a Leco C744 carbon analyzer. The samples were pretreated with hot 18% HCl to remove carbonates. Powdered rock samples were subjected to pyrolysis on Rock Eval 6 (Espitalié et al., 1985; Espitalié and Bordenave, 1993). The main Rock-Eval parameters are: S_1 – the amount of free hydrocarbons; S_2 – the amount of hydrocarbon generated through thermal cracking; S_3 – the amount of CO_2 produced during pyrolysis; T_{max} – the temperature at maximum release of hydrocarbons; hydrogen index ($HI=S_2 \times 100/TOC$), oxygen index ($OI=S_3 \times 100/TOC$), production index ($PI=S_1/(S_1+S_2)$); MINC – mineral carbon.

Organic petrography, including vitrinite reflectance (VR), was performed following established procedures (Stach et al., 1982; Taylor et al., 1998). Selected samples (based on TOC content >0.25 wt.%) were examined microscopically using organic matter concentrate obtained after $HCl/HF/ZnCl_2$ treatment of rock. Organic matter was examined and photographed in transmitted and blue-fluorescent light on an Olympus BX-51 microscope, and in reflected light on a Zeiss Axio Imager microscope equipped with an MSP 210 microscope spectrometer.

Vitrinite reflectance ($\%R_o$, random reflectance values, including the number of measurements and standard deviation) was measured using oil immersion (50x objective) in incident non-polarized light at 546 nm. Calibration was performed using standards with known reflectance values (Spinel, Sapphire, Yttrium-Aluminum-Garnet). An internal conversion scale was used to correlate the Thermal Alteration Index (TAI) with VR ($\%R_o$). The thermal alteration index (TAI) 3 corresponds to 0.95–1.25%R_o and 3^+ to 1.25–2%R_o. Maceral descriptions followed the classifications presented in Stach et al. (1982) and Taylor et al. (1998).

4. Lithostratigraphy

4.1. Lithofacies description

The measured section is around 19 m thick and comprised of conformably deposited thin-bedded, laminated or massive dolostone, limestone, chert, tuff and limestone breccia beds (Fig. 3). The beds are usually planar, tabular with sharp contacts (Figs. 4b, d and e). The only exception is seen as the irregular upper bedding plane of the limestone breccia bed. A large fragment of *Equisetites* was observed in the upper part of the succession (Figs. 4b and c).

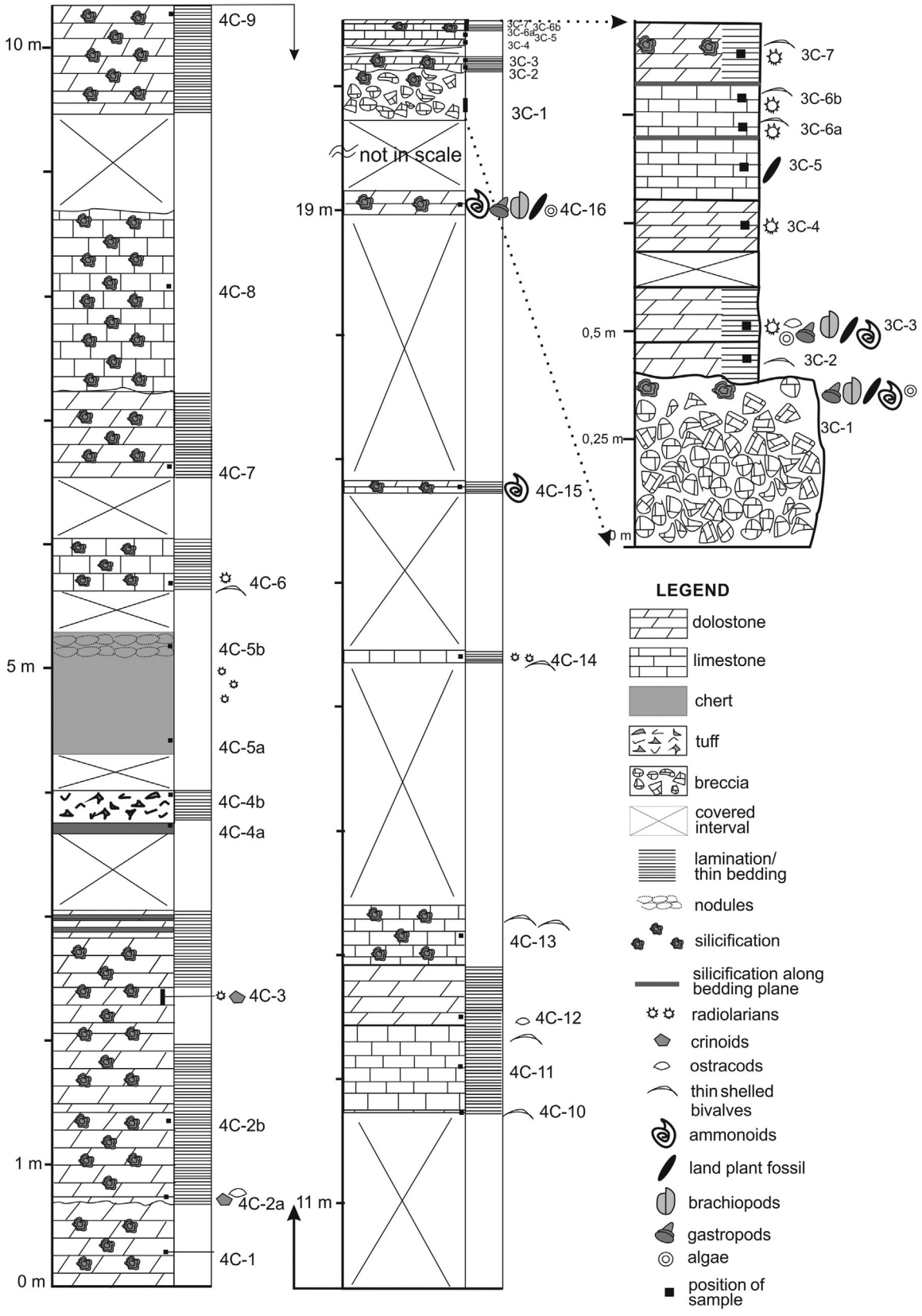

Fig. 3. Stratigraphic log of the measured section and position of samples (position within the local Triassic succession is indicated in Fig. 2).

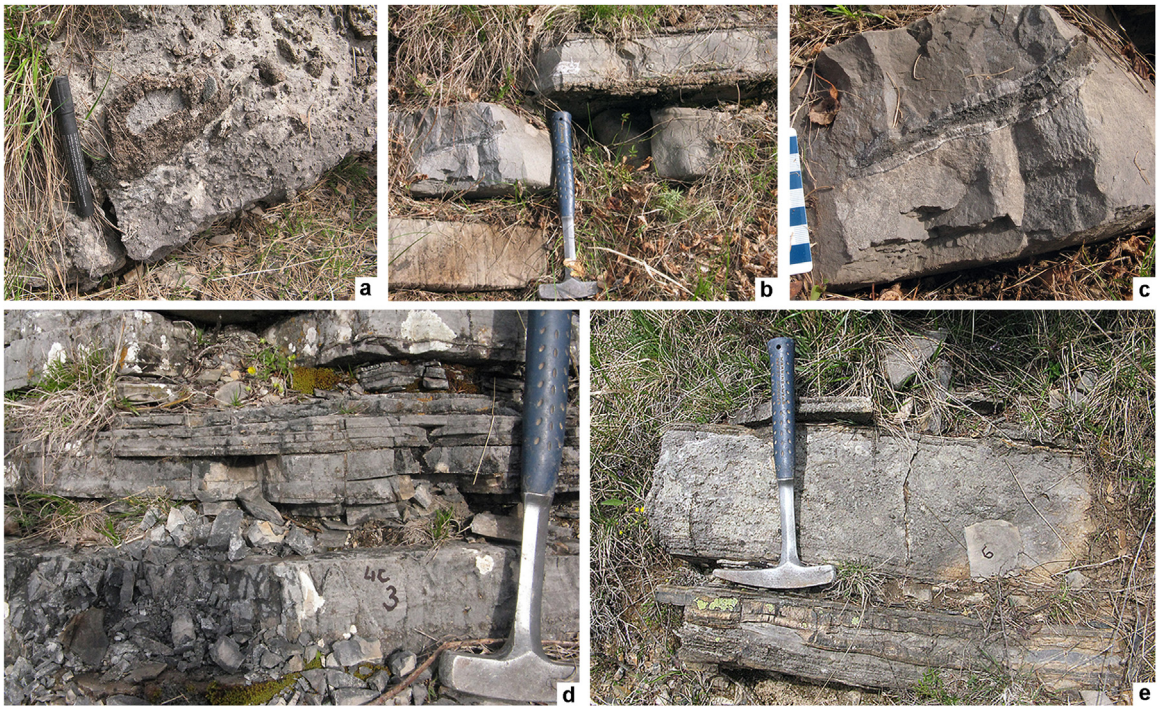

Fig. 4. Field photos of the section in Fig. 3. **(a)** Strongly silicified limestone breccia bed near the top of the section. **(b)** Bedded limestone 1 m above the breccia. Note silicification in the lower and upper beds, and *Equisetites* in the middle bed. **(c)** Detail of b) focused on the *Equisetites* stem. **(d, e)** Thin-bedded partly dolomitized limestone with laminae of replacement chert (lower part of the section, samples 4C-3 and 4C-6).

Dolostone has a macrocrystalline polymodal or homogeneuous s-type (subidiotopic) texture (Fig. 5a). Primary constituents are faintly preserved or not preserved at all. Among the faintly preserved primary components, bioclasts (crinoids, radiolarians, thin-shelled bivalves, ostracods, rare algae) and lithoclasts can be differentiated. Diagenetic silicification was commonly observed (Figs. 4a, b, d, e, Fig. 5a). In the considerably silicified dolostone, colloid silica forms are present (sample 4C-2b). In the uppermost part of the succession, silicification was observed along the bedding planes. Dolomitized radiolarians are occasionally present (Fig. 5b).

Limestone corresponds to severely recrystalized grainy limestone types. They consist of limy fragments that are determined as lithoclasts (Fig. 5c). In places, lithoclasts composed of pellets and intraclasts cemented by sparry calcite are present. Subordinately, bioclastic fragments of crinoids, radiolarians, thin-shelled bivalves (Fig. 5d), ostracods, and rare ammonoids are present. Primary (limestone) constituents were subsequently dolomitized. Irregular, nodular, and lenticular silicification can be substantial.

Tuff layers are presented by vitriclastic tuff types (Fig. 5e). The tuff consists of very fine- to medium-sized ash fragments presented by shards. The shards exhibit bubble-wall, needle-like, cuspate or “y”-shaped forms. Subordinately coarse grained crystalloclasts of quartz, feldspar (plagioclase, sanidine), and biotite are concentrated at the base of the tuff (Fig. 5f).

Chert dominantly consists of fine crystalline quartz crystals and often contains a subordinate amount of carbonate minerals (Fig. 5g, h). Calcitized radiolarians can rarely be seen. In the middle of the section (~ 5 m from the base), the chert bed exhibits nodule-like forms.

The breccia bed near the top of the section (Fig. 3) consists of cm-sized subrounded limestone clasts and carbonate matrix. The breccia bed exhibits grading as its upper part is composed of fine-grained carbonate detritus. This part is also significantly silicified (Fig. 4a).

4.2. Organic matter characterization

The 19 analyzed samples exhibit a total organic carbon (TOC) content ranging from 0.03 to 0.50 wt.% (Table 1, Fig. 6). While cherts and tuffs generally exhibit low TOC, carbonate-rich samples (45–65% carbonate) tend to have slightly higher values. Microscopic examination of isolated kerogen from samples with TOC >0.24% revealed predominantly amorphous, dark, and non-fluorescent organic matter with traces of vitrinite, inertinite (fusinite), and pyrobitumen particles, indicating a high degree of thermal alteration (Fig. 7; Stach et al., 1982, Taylor et al., 1998). The carbonates are without generative potential and source rock characteristics. The low hydrogen index suggests a kerogen type III and IV (Peters and Cassa, 1994). Optical maturity parameters (R_o 1.28–1.52%, TAI 3 to 3^+) and maximum pyrolysis temperature (T_{max} >460 °C) indicate a high level of thermal maturity (Table 1). The advanced stage of thermal alteration makes it difficult to precisely determine the original nature of the organic matter. The presence of vitrinite particles points to a terrestrial input, classifying the organic matter as kerogen type III. However, the potential presence of pyrobitumen suggests a mixed kerogen type (II/III), which is more characteristic of deeper marine, oxygen-deficient environments like intraplatform basins. Carbonate-rich samples from these basins, with higher organic matter content, may have had some petroleum potential in the past (Zappaterra, 1994).

5. Conodonts

5.1. Description of the conodont fauna

The recovered conodont fauna is well preserved. The specimens are black in color and have a Conodont Alteration Index (CAI) between 5 and 5.5 (Epstein et al., 1977). Next to conodont elements, rare fish remains and crinoid ossicles are encountered. One sample (3C-6 – inv. No GeoZS 5760) is particularly rich in radiolarians.

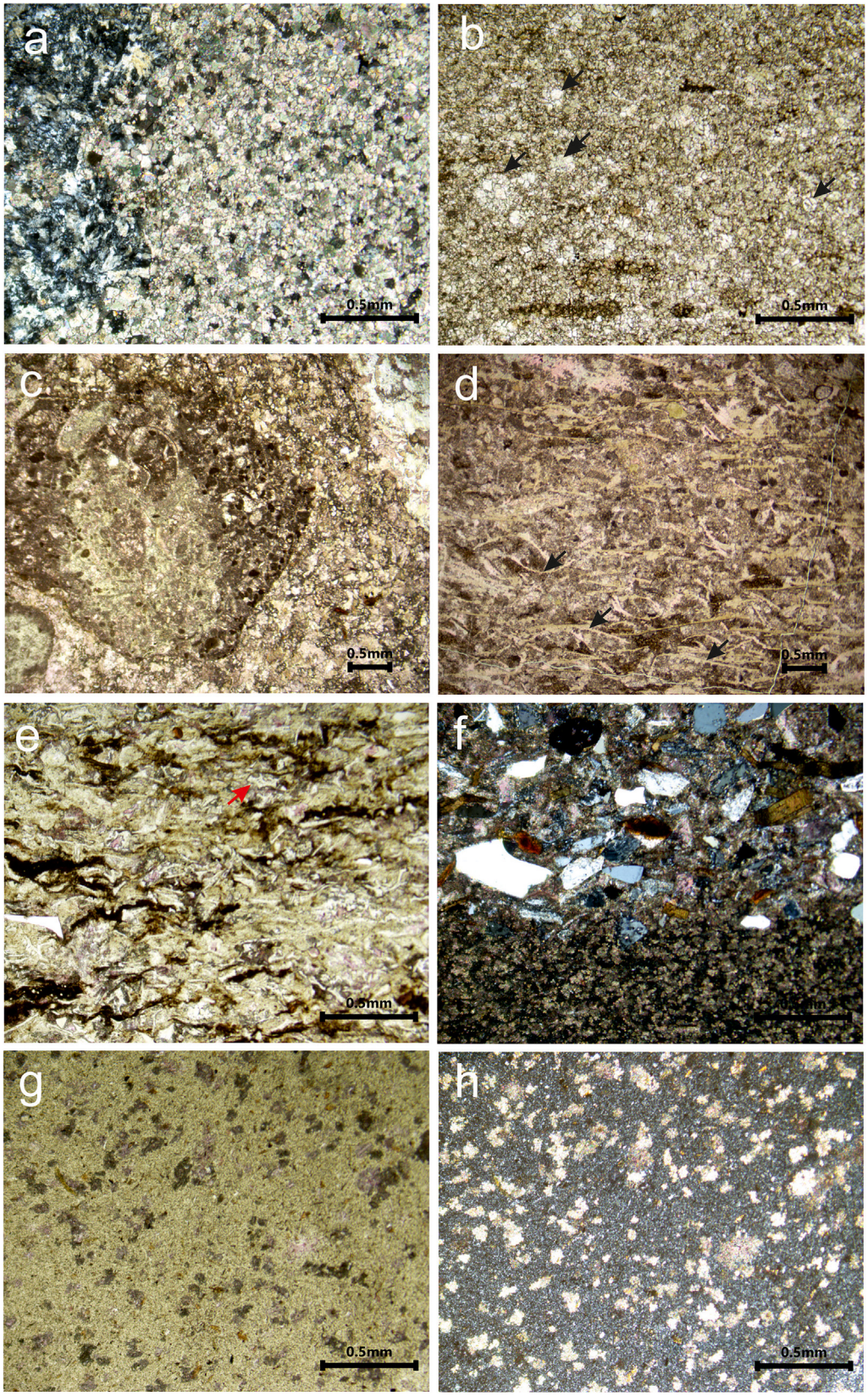

Fig. 5. Sedimentary rock types from the measured section. (a) Macrocrystalline texture of dolostone (subidiotopic), intense silicification on the left; crossed nicols, sample 4C-2b). (b) Macrocrystalline dolostone with faintly preserved dolomitized radiolarians (arrows); (sample 3C-7). (c) Severely recrystallized limestone with preserved resedimented lithoclast (sample 4C-8). (d) Recrystallized limestone with thin-shelled bivalves (arrows) (sample 4C-13). (e) Vitriclastic tuff with various shard forms; the arrow points to the bubble-wall fragment (sample 4C-4b). (f) Crystalloclastic material accumulated sometimes at the base of a vitriclastic tuff bed in contact with the underlying chert bed; crossed nicols; (sample 4C-4a). (g, h) Homogenous microtexture in the patchy calcitized chert; parallel (g) and crossed (h) nicols; (sample 4C-5a).

Table 1
Total organic carbon content (TOC), rock eval pyrolysis data, vitrinite reflectance and thermal alteration index (TAI) of Mt. Svilaja samples.

Sample	TOC_{Leco} (%)	TOC_{RE} (%)	S_1 mgHC g rock	S_2 mgHC g rock	S_3 mg CO_2 g rock	T_{max} (^{0}C)	HI mgHC g TOC	OI mgCO_2 g TOC	PI	S_2/S_3	MINC %	%R_o	TAI
3C-2	0,13	0,11	0,00	0,03	0,57	444	27	518	0,01	0,05	9,39		
3C-3	0,50	0,35	0,02	0,13	0,41	448	37	117	0,12	0,32	9,55	1,52	3^+
3C-4	0,31	0,23	0,02	0,07	0,32	445	30	139	0,17	0,22	9,97	1,50	3^+
3C-5	0,35	0,30	0,05	0,11	0,15	473	37	50	0,32	0,73	6,99		3^+
3C-6A	0,40	0,29	0,08	0,11	0,28	465	38	97	0,42	0,39	7,48	1,42	3^+
3C-6B	0,42	0,36	0,09	0,15	0,08	481	42	22	0,36	1,88	6,25	1,34	3^+
3C-7	0,17	0,25	0,01	0,04	0,54	464	16	216	0,13	0,07	10,27		
4C-2A	0,08	0,05	0,00	0,01	0,08	471	20	160	0,00	0,13	9,69		
4C-2B	0,25	0,20	0,01	0,05	0,18	471	25	90	0,18	0,28	10,00	1,28	$3–3^+$
4C-3	0,24	0,22	0,03	0,05	0,07	472	23	32	0,38	0,71	10,20		3^+
4C-4A	0,05	0,04	0,00	0,00	0,16	430	0	400	0,72	0,00	3,14		
4C-4B	0,16	0,20	0,03	0,05	0,58	469	25	290	0,36	0,09	1,22		
4C-5A	0,04	0,01	0,00	0,00	0,05	482	0	500	0,00	0,00	0,74		
4C-5B	0,03	0,07	0,00	0,00	0,06	488	0	86	0,00	0,00	2,50		
4C-6	0,35	0,40	0,04	0,17	0,73	475	42	182	0,18	0,23	5,85		3^+
4C-7	0,20	0,14	0,01	0,03	0,18	463	21	129	0,19	0,17	7,68		
4C-9	0,18	0,13	0,00	0,02	0,20	464	15	154	0,00	0,10	9,87		
4C-12	0,19	0,17	0,00	0,03	0,27	470	18	159	0,06	0,11	9,99		
4C-16	0,11	0,14	0,00	0,04	0,15	441	29	107	0,03	0,27	9,39		

TOC total organic carbon content, Rock Eval pyrolysis data: S_1 the amount of free hydrocarbons, S_2 the amount of hydrocarbon generated through thermal cracking, S_3 the amount of CO_2 produced during pyrolysis, T_{max} the temperature of maximum hydrocarbon generation, PI Production index, (Peters and Cassa,1994), %R_o Vitrinite reflectance; TAI Thermal alteration index, TAI 3 = 0,95–1,25%R_o; TAI 3^+= 1,25–2%R_o.

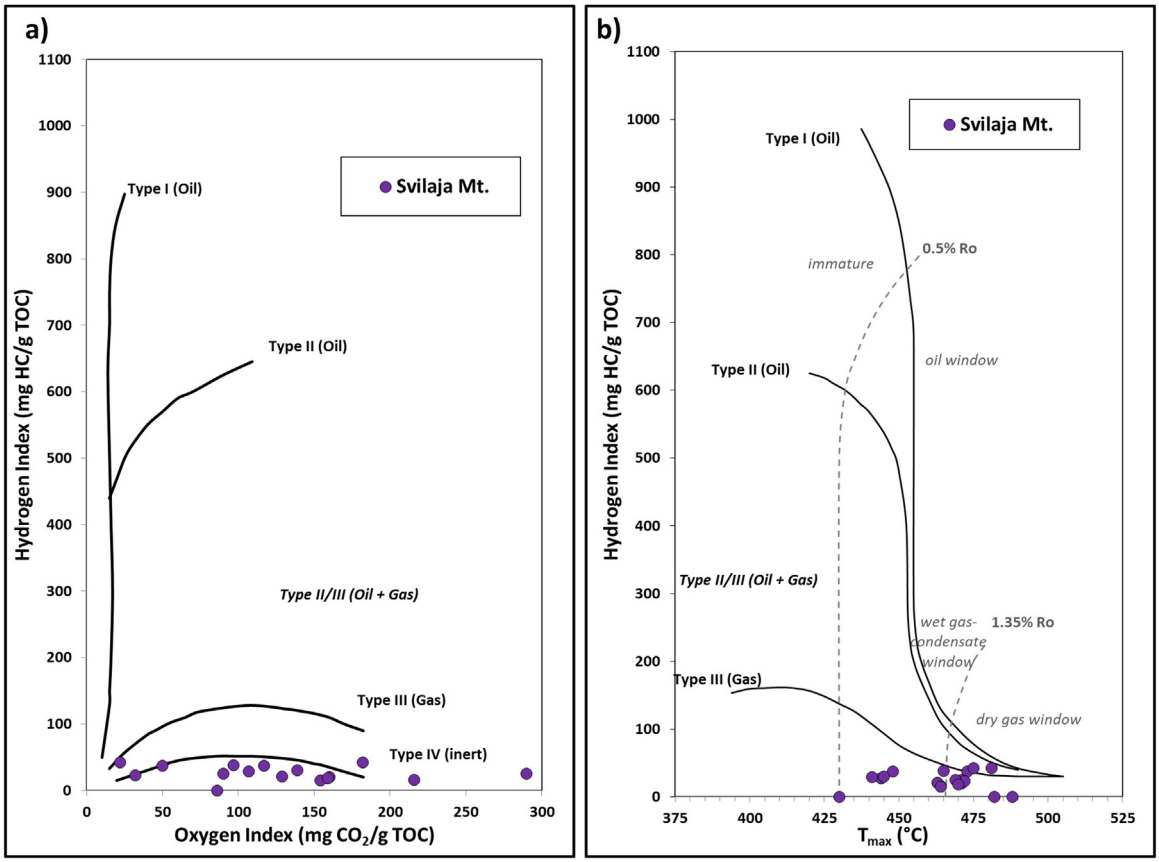

Fig. 6. (a) Modified Van Krevelen diagram (Hydrogen index (HI) versus Oxygen index (OI)) crossplot showing organic matter type distribution. (b) Hydrogen index (HI) versus T_{max} crossplot illustrating thermal maturity trends.

Most collections are marked by the presence of *Budurovignathus hungaricus* (Kozur and Végh) (in Kozur and Mock, 1972), which is frequently joined with *Paragondolella alpina* (Kozur and Mostler, 1982a) or *Paragondolella* ex gr. *alpina*, whereas other accompanying conodont taxa are: *Budurovignathus* sp., *Gladigondolella* sp., *Ozarkodina* sp., *Paragondolella trammeri* (Kozur, 1972), *Paragondolella* ex gr. *trammeri* and *Paragondolella* sp. (Table 2, Fig. 8).

The elements of *B. hungaricus* have a full-length platform with no ornamentation that tapers toward the anterior and posterior margin and attains its greatest width in the median part. The massive platform has

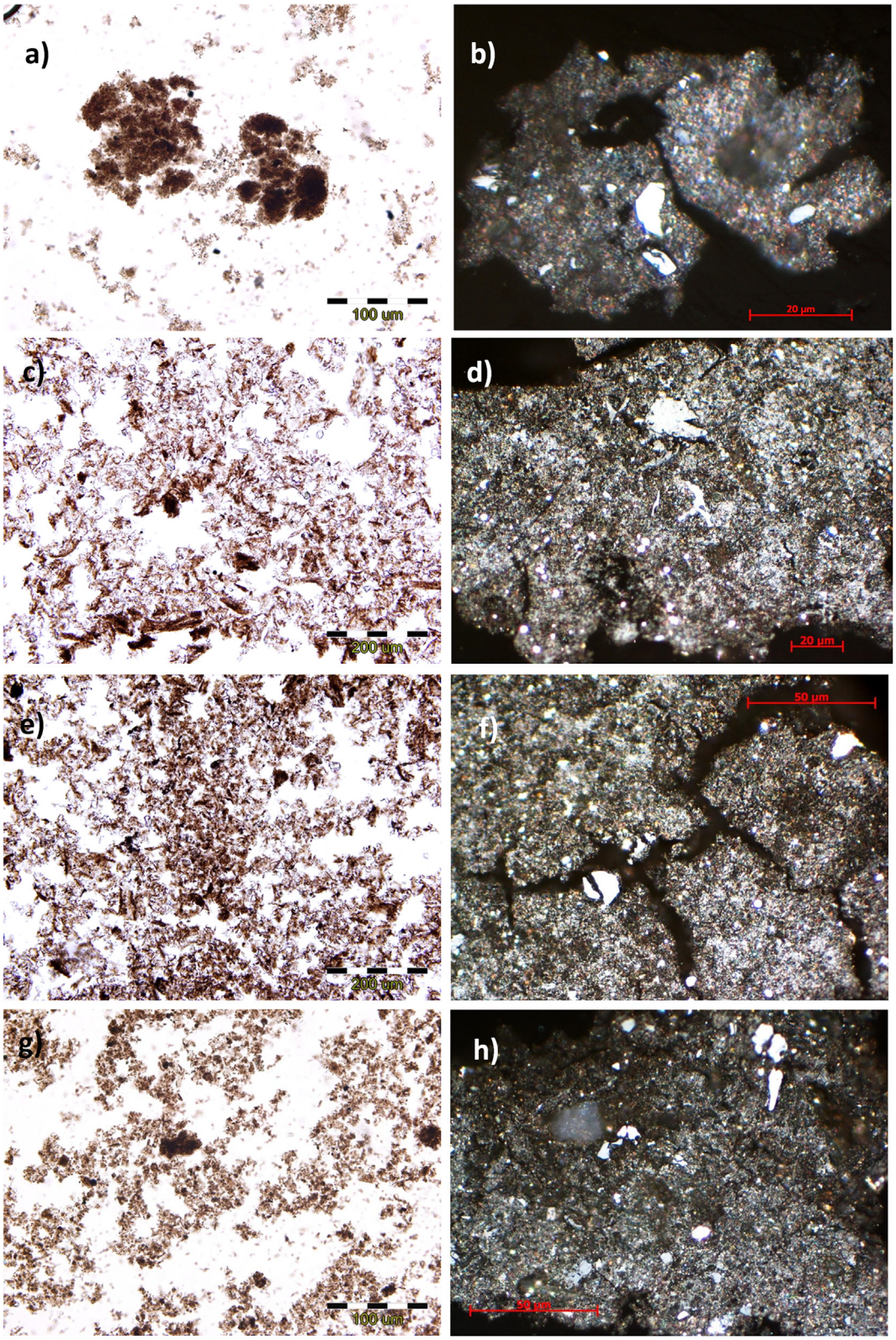

Fig. 7. Photomicrographs of Svilaja 3C-3 (a, b); Svilaja 3C-6a (c, d); Svilaja 3C-6b (e, f), Svilaja 4C-3 (g, h) showing thermally altered amorphous organic matter with traces of vitrinite particles (1.28 to 1.52%R_o). Transmitted light (left), Reflected light, oil immersion (right).

Table 2
Distribution of conodont taxa in the investigated section.

Conodont taxa	Sample number								
	4C-2B	4C-3A	4C-3B	4C-6	4C-7	4C-8	3C-4	3C-5	3C-6
Budurovignathus hungaricus	1	1	1					14	3
Budurovignathus sp.					1	1			
Gladigondolella sp.	1	1							
Ozarkodina sp.							1		
Paragondolella alpina			1			5		5	
Paragondolella ex. gr. *alpina*	8								7
Paragondolella trammeri								5	3
Paragondolella ex. gr. *trammeri*	4								5
Paragondolella sp.	10			1	1		1	3	4
ramiform elements (fragm.)	1		7		3	12	4	12	11

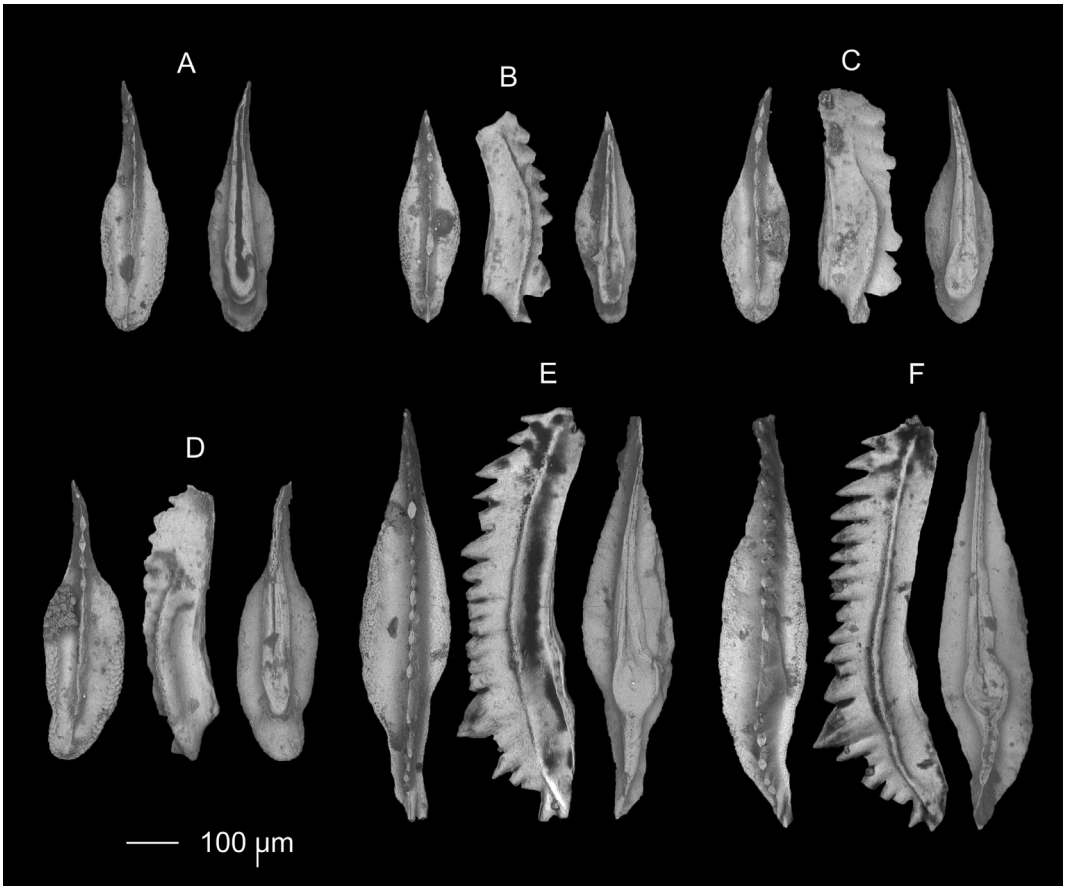

Fig. 8. Conodonts from the Svilaja section, *hungaricus* Zone, Ladinian (Fassanian).
A *Paragondolella alpina* (Kozur and Mostler, 1982a). Sample 3C-5 (GeoZS 5759).
B *Paragondolella* ex gr. *trammeri* (Kozur, 1972). Sample 3C-6 (GeoZS 5760).
C *Paragondolella* sp. Sample 3C-6 (GeoZS 5760).
D *Paragondolella alpina* (Kozur and Mostler, 1982a). Sample 3C-5 (GeoZS 5759).
E, F *Budurovignathus hungaricus* (Kozur and Végh) *in* Kozur and Mock (1972). Sample 3C-5 (GeoZS 5759).

a sigmoidal bent in the position of a prominent cusp. The carina is high and composed of 16–21 denticles. The lower side is marked by a keel with notable and forward-shifted basal cavity consisting of two small pits connected by a short furrow. The latter is ovaloid, but in some specimens it is quite wide and nearly rounded. Behind the loop, the keel tapers gradually and in the posterior part it is reduced to a ridge that ends in the posterior tip.

The recovered specimens reveal typical budurovignathid features on the upper surface. However, on the lower surface of some specimens, a circular loop of the neogondolellid ancestor is retained, although it is forward-shifted and a prominent keel is developed behind it. The posterior platform in only a few specimens is wide with an angular posterior margin which is unlike the pointed posterior margin in most budurovignathids. While the origin of *Budurovignathus* has still to be explained, the material from Svilaja suggests its neogondolellid ancestors, which is in the line with the origin from *Neogondolella aequidentata* Kozur, Krainer and Lutz via *B. praehungaricus* (Orchard, 2010).

P. trammeri (Kozur, 1972) is characterized by small to medium units whose width is greatest in the middle. It is worth mentioning the observation of the author of this species that stratigraphically younger forms have a reduced platform in the anterior third; the stratigraphically older forms lack this reduction (Kozur, 1972). The considerably high carina

is slightly lower in the middle part. A quite wide cusp is present before the last denticle; it is followed by the last denticle which is fused with the platform end. The keel is high with a significantly wide loop with the position of a long and large basal pit.

P. alpina (Kozur and Mostler, 1982a) is represented by small to medium units with a reduced platform and a free blade. The carina is high and is mostly fused in adults. The last two denticles are somewhat stronger and stand separated, the last one is usually fused with the posterior end. The platform is widest in the anterior half with parallel margins, becomes narrower posteriorly, and forms a rounded end. As a rule, the posteriormost narrower platform portion reveals a slight bend to the side.

P. alpina and *P. trammeri* are closely related (Kozur and Mostler, 1982a; Kovács, 1994; Chen et al., 2016). The two species are mainly distinguished by a shorter platform and narrow keel that only slightly widens posteriorly in the area of the basal pit in *P. alpina*. Moreover, in the studied material the last denticle is generally the largest in *P. alpina*.

5.2. Conodont biostratigraphy

Budurovignathus is a typical Ladinian genus, although a few representatives are known from the lowermost Carnian strata. Species *B. hungaricus* ranges from the Fassanian to the Middle Longobardian. It was first described from Felsőörs, Hungary, in strata assigned to the Lower Longobardian (Kozur and Mock, 1972). In Epidaurus, Greece, it was reported from the *Curionii, Gredleri* and *Archelaus* Ammonoid Zones where it occurs in association with *Gladigondolella tethydis, B. japonicus, Neogondolella* cf. *constricta, P. excelsa, P. trammeri* and, in the upper part of its range, also with *B. mungoensis*. In addition, it is the marker of the Fassanian *hungaricus* Zone that is found in the standard conodont zonation (Ogg et al., 2016), and in the conodont zonation of Slovenia (Kolar-Jurkovšek and Jurkovšek, 2019).

P. trammeri is a well-known Middle Triassic species that has been established from the *Curionii* Ammonoid Zone of Köveskal, Hungary (Kozur and Mock, 1972), whereas *Paragondolella alpina* was first described from the platy limestone with *Parakelnerites* of the *Reitzi* Ammonoid Zone of the Gailtal Alps (Kozur and Mostler, 1982a). In Epidaurus, *P. trammeri* co-occurs with *Budurovignathus hungaricus* throughout its range, however, *Paragondolella trammeri* in this section appears already in the *Nevadites secedensis* Ammonoid Zone and is present up to the top of the *Archelaus* Zone (Krystyn, 1983). In the Bagolino section, Italy, the strata of the *N. secedensis* Zone are marked with the conodont association yielding *P. alpina* group, *P.* aff. *eotrammeri, P. fuelopi, P. trammeri,* whereas *B. hungaricus* was found in a higher level of the section (Brack and Nicora, 1998; Brack et al., 2005). The three species (*B. hungaricus, P. alpina, P. trammeri*) co-occur in the *Curionii* Zone of the Balaton Highland where full pelagic conditions are indicated by the presence of gondolellids (Kovács, 1994). *P. alpina* and *P. trammeri* appear to be confined to Tethyan sections and where most budurovignathids are common (Orchard, 2010).

The Ladinian age of the studied strata is defined by the occurrence of *Budurovignathus hungaricus* that appears in association with *P. alpina* and *P. trammeri*. The strata are attributed to the Fassanian *hungaricus* conodont Zone where it appears in the absence of *B. mungoensis*.

6. Radiolaria

6.1. Taxonomic structure and biostratigraphy

Determinable radiolarians were found in samples 4C-6 and 3C-6 (Fig. 3). They are rare in sample 4C-6 but more abundant and moderately well preserved in sample 3C-6. The diversity in both samples is very low (Table 3, Pls. 1–3). Nineteen genera have been identified in total. Sample 3C-6, which is more complete, contains 19 species assigned to 16 genera. Seven genera belong to Entactinaria, five to Spumellaria and four to Nassellaria. Specimens of spherical Entactinaria and Spumellaria with spongy and also latticed shells prevail but Nassellaria are very rare. They constitute <5% of all radiolarian specimens and are composed almost exclusively of monocyrtids, among which only *Hozmadia* is relatively common. Very rare monaxone and triaxone sponge spicules are associated.

Stratigraphic evaluation of this radiolarian fauna is difficult because age diagnostic taxa for the interval around the Anisian–Ladinian boundary are missing. The index species in the zones and subzones of Kozur and co-workers (Kozur and Mostler, 1994; Kozur et al., 1996; Kozur, 2003) are representatives of multicyrtid Nassellaria (*Spongosilicarmiger, Ladinocampe*) and Oertlispongidae, but none of those is present in the samples from Mt. Svilaja. Stockar et al. (2012) compiled stratigraphic ranges for species which they encountered in the Lower Ladinian San Giorgio Dolomite. Among species found at Mt. Svilaja, *Pseudostylosphaera tenuis* (Nakaseko and Nishimura), *Triassospongosphaera multispinosa* (Kozur and Mostler), *Spongopallium* aff. *koppi* (Lahm), *Poulpus curvispinus* Dumitrica, Kozur and Mostler, *Hozmadia reticulata* Dumitrica, Kozur and Mostler, and *Archaeocenosphaera igoi* (Sashida) (=*Archaeospongosphaera* sp. B *in* Stockar et al., 2012) are considered in their range chart. All these species (except *Archaeocenosphaera*, which is too simple to be a reliable stratigraphic marker) range at least from the Upper Anisian *Spongosilicarmiger italicus* Radiolarian Zone (i.e., from the *Reitziites reitzi* Ammonoid Zone) to the end of the Ladinian. It is, however, worth noting that no *Muelleritortis* species occur in the Svilaja section even though genera of the closely related Hindeosphaeridae (*Pseudostylosphaera, Parasepsagon*) are common. Further, *Muelleritortis* is known not only from oxic facies but also from dark bituminous limestone (Kolar-Jurkovšek et al., 2023). Hence, the absence of *Muelleritortis* is more probably related to the age than to ecological factors, meaning that radiolarians from Mt. Svilaja are older than the upper Fassanian *Muelleritortis firma* and the Longobardian *Muelleritortis cochleata* zones of Kozur (2003). This inference is in line with the precise conodont dating to the Fassanian *Budurovignathus hungaricus* Zone.

6.2. Radiolarian systematics

Published data on several species found at Mt. Svilaja are very scarce, although the Anisian–Ladinian interval has been extensively investigated for nearly 50 years. Some species were described decades ago but have never been or only very rarely documented in later works. A basic synonymy is thus provided for all taxa and remarks are added where necessary. The assignment to families and genera follows O'Dogherty et al. (2009) and Stockar et al. (2012). Type species of genera are presented in these two publications and are omitted here.

Class RADIOLARIA Müller, 1858
Subclass POLYCYSTINEA Ehrenberg, 1839
Order ENTACTINARIA Kozur and Mostler, 1982b
Family PENTACTINOCARPIDAE Dumitrica, 1978b
Genus ***Pentactinocarpus*** Dumitrica, 1978b

Pentactinocarpus tetracanthus Dumitrica, 1978b

Plate 2, figs. 1–3

1978b *Pentactinocarpus tetracanthus* n. sp. – Dumitrica, p. 44, pl. 2, fig. 1.
2015 *Pentactinocarpus tetracanthus* Dumitrica – Ozsvárt et al., p. 345, Fig. 5.11–5.13 (and the synonymy therein).

Genus ***Pentactinocapsa*** Dumitrica, 1978b

Pentactinocapsa quadripes Dumitrica, 1978b
Plate 2, fig. 4

1978b *Pentactinocapsa quadripes* n. sp. – Dumitrica, p. 45, pl. 1, figs. 2–4 .

Table 3
Occurrence of radiolarian taxa in the studied samples.

Species Samples	4C-6	3C-6
Archaeocenosphaera igoi (Sashida)		X
Archaeocenosphaera sp. C *sensu* Lahm 1984		X
Bernoulliella sp.	X	
"Entactinosphaera" cf. *simoni* Kozur and Mostler		X
Hozmadia reticulata Dumitrica, Kozur and Mostler	X	X
Lobactinocapsa ellipsoconcha Dumitrica gr.		X
Neopylentonema sp. A		X
Parasepsagon longobardicus (Kozur and Mostler)	X	X
Parentactinosphaera cf. *fassanensis* (Kozur and Mostler)		X
Paurinella mesotriassica Kozur and Mostler		X
Pentactinocapsa quadripes Dumitrica		X
Pentactinocarpus tetracanthus Dumitrica		X
Pessagnollum? aff. *hexaspinosum* Stockar, Dumitrica and Baumgartner	X	
Poulpus curvispinus Dumitrica, Kozur and Mostler		X
Poulpus oertlii (Kozur and Mostler)		X
Pseudostylosphaera tenuis (Nakaseko and Nishimura)	X	X
Pyramicyrtium? sp.		X
Spongopallium aff. *koppi* (Lahm) *sensu* Tekin and Sönmez 2010	X	X
Thaisphaera minuta Sashida and Igo	X	
Tiborella sp.		X
Triassospongosphaera multispinosa (Kozur and Mostler)	X	X
Triassospongosphaera? spp.		X

2023 *Pentactinocapsa quadripes* Dumitrica – Ozsvárt et al., p. 18, pl. 1, fig. 3 (and the synonymy therein).

Genus ***Lobactinocapsa*** Dumitrica, 1978b

Lobactinocapsa ellipsoconcha Dumitrica, 1978b group
Plate 1, figs. 1–7, ?8, 9–18

1978b *Lobactinocapsa ellipsoconcha* n. sp. – Dumitrica, p. 49, pl. 3, figs. 1–2; pl. 4, fig. 3.
2011 *Lobactinocapsa* cf. *ellipsoconcha* Dumitrica – Velledits et al., fig. 20/13.

Remarks: Lobactinocapsa has a very scarce record in radiolarian literature. Three species of this genus have been described thus far: *L. ellipsoconcha* Dumitrica (1978b), *L. bilobata* Dumitrica (1978b), and *L. carnica* Kozur and Mostler (1981). The type species *L. ellipsoconcha* has only been reported once after the original description (see the synonymy) and the record of the two other species is limited to the original descriptions. The genus may be indeed rare, yet in rich and well-preserved samples it might simply be overlooked due to its indistinct external appearance. Spongy spheroidal radiolarians are generally considered to be stratigraphically insignificant and thus are often neglected in routine radiolarian research.

Lobactinocapsa is the most abundant genus in sample 3C-6 from Svilaja. Several broken specimens were found that allow easy observation of the inner as well as outer structure. The inner shell of all broken specimens consists of an apical pentactine spicule, which continues downwards into a loosely latticed chamber and on the opposite side is covered by a bilobate, latticed cap (Pl. 1, fig. 2). The cortical shell is much more variable. The shape varies from ovoid (Pl. 1, fig. 11) to almost spherical (Pl. 1, figs. 14, 15). The wall thickness varies from a thin single layer (Pl. 1, figs. 1, 2) to a thick spongy meshwork (Pl. 1, fig. 10). The external spines can be faint and rare (Pl. 1, figs. 4a–b) or strong and numerous. Some specimens bear 20 or more, stout conical spines (Pl. 1, figs. 14, 15, 16). Since there are no clear limits among different morphologies and all specimens originate from the same sample, we consider them as a group assignable to *L. ellipsoconcha* Dumitrica. Some specimens are close to the holotype of *L. ellipsoconcha* (pl. 3, fig. 2 in Dumitrica, 1978b, compare Pl. 1, fig. 9 herein), some others are closer to the paratype (pl. 3, fig. 1 in Dumitrica 1978b, Pl. 1, fig. 13 herein) whereas many specimens are quite different from both the holotype and the paratype (Pl. 1, figs. 4a–b, 6–7, 14–16).

Although we broaden the definition of *L. ellipsoconcha* to a group, we still consider *L. bilobata* Dumitrica and *L. carnica* Kozur and Mostler as a separate species. *L. bilobata* is distinguished by having a free initial skeleton without a cortical shell. *L. carnica* has a bigger number of connecting spines between the inner skeleton and the cortical shell.

The spherical specimens with >10 spines are externally similar to *Astrocentrus* Kozur and Mostler, and to *Triassospongosphaera* Kozur and Mostler but the spines are always much shorter. These specimens are closely similar to *Norispongus poetschensis* Kozur and Mostler (1981, p. 46, pl. 48, figs. 1–3) and especially to *Norispongus*? *goestlingensis* Kozur and Mostler (1981, p. 47, pl. 3, fig. 3) that have very short spines. *Norispongus* Kozur and Mostler (1981), whose inner structure is not known, was tentatively synonymized with *Triassospongosphaera* by O'Dogherty et al. (2009). It is equally possible that *Norispongus* belongs to *Lobactinocapsa* or another genus of Pentactinocarpidae.

Double skeletons also exist in sample 3C-6 (Pl. 1, fig. 8). Three such specimens were found, all with a recrystallized interior. Even though the assignment to *Lobactinocapsa* is thus questionable, it is still the most likely because comparable single skeletons of *Lobactinocapsa* (Pl. 1, fig. 7) are common. Such "Siamese twins" (De Wever, 1985; Dumitrica, 2013) or "conjoined skeletons" (Itaki and Bjørklund, 2008) are rare but known in sediments of various ages and have been considered as supportive evidence for the asexual reproduction of radiolarians by binary fission. The twinned skeletons formed when the two progeny individuals were not completely separated but shared the same ectoplasm in which the joint skeleton was built (see De Wever, 1985; Itaki and Bjørklund, 2008; Dumitrica, 2013, for a detailed explanation and discussion).

Family MULTIARCUSELLIDAE Kozur and Mostler, 1979
Subfamily **AUSTRISATURNALINAE** Kozur and Mostler, 1983
Genus ***Tiborella*** Dumitrica, Kozur and Mostler, 1980

***Tiborella* sp.**
Plate 2, fig. 5

Remarks: Only rare fragments of *Tiborella* were found and could not be determined at species level.

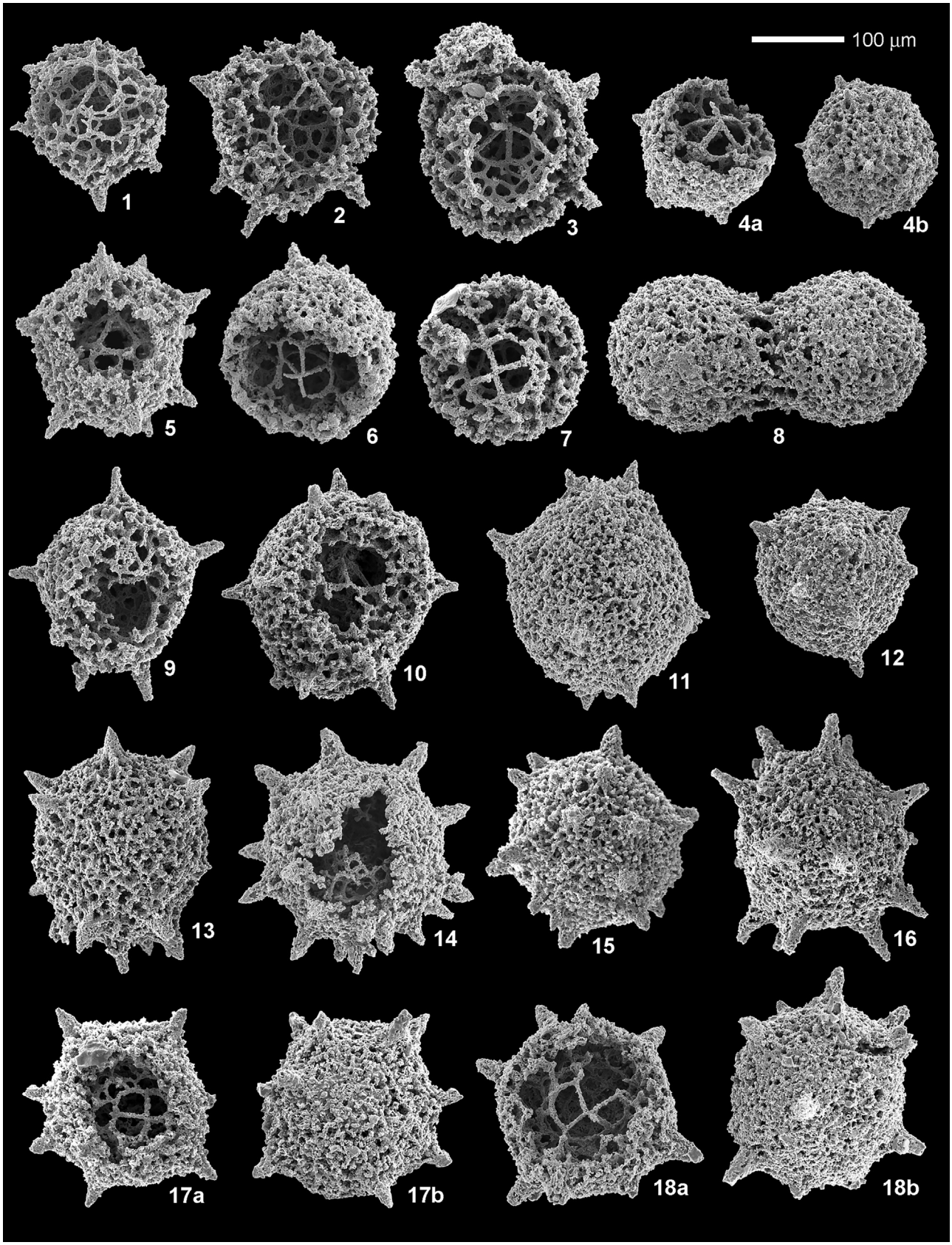

Plate 1. 1–18. *Lobactinocapsa ellipsoconcha* Dumitrica gr.; 1, 2, 5, 9, 10 – inner structure in a lateral view; 3 – inner structure in an oblique basal view; 4a, 6, 7, 17a, 18a – inner structure in an oblique apical view; 8 – "Siamese twins"; 4b, 17b, 18b – same specimens as 4a, 17a, 18a respectively, rotated 180° around the vertical axis of the photograph. All specimens are from sample 3C-6. Scale bar 100 µm for all figures.

Family HEPTACLADIDAE Dumitrica, Kozur and Mostler, 1980
Genus ***Parentactinosphaera*** Kozur and Mostler, 1979

Parentactinosphaera* cf. *fassanensis (Kozur and Mostler, 1981)

Plate 2, figs. 6–10

cf. 1981 *Weverisphaera fassanensis* n. sp. – Kozur and Mostler, 34, pl. 68, figs. 1a and b.
cf. 1984 *Weverisphaera fassanensis* Kozur and Mostler – Lahm, 37, pl. 5, fig. 10.
cf. 1995 *Weverisphaera fassanensis* Kozur and Mostler – Kellici and De Wever, 163, pl. 6, fig. 10.

Remarks: This species is quite common but poorly preserved in the studied material. The cortical shell is partly dissolved and the spines are often broken. No complete specimen has been found. Externally, this species is similar to *Bernoulliella* but has seven spines (not six) and the arrangement of the spines, best visible in Pl. 2, fig. 8, is typical of Heptacladidae. *Weverisphaera* Kozur and Mostler is considered a junior synonym of *Parentactinosphaera* Kozur and Mostler (O'Dogherty et al., 2009; for further remarks on the genus, see Stockar et al., 2012).

Family HINDEOSPHAERIDAE Kozur and Mostler, 1981
Genus ***Pseudostylosphaera*** Kozur and Mostler, 1981

Pseudostylosphaera tenuis (Nakaseko and Nishimura, 1979)
Plate 2, figs. 11–17

1979 *Archaeospongoprunum tenue* n. sp. – Nakaseko and Nishimura, p. 68, pl. 1, figs. 8, 10.
2012 *Pseudostylosphaera tenuis* (Nakaseko and Nishimura) – Stockar et al., p. 397, pl. 4, figs. 8–15 (and the synonymy therein).

Remarks: The three-spined specimen (Pl. 2, fig. 17) is considered an anomaly of *P. tenuis*. The number of spines evokes the genus *Sepsagon* Dumitrica, Kozur and Mostler, but the additional spine (arising from one of the apical spines of the inner skeleton?) is much thinner than the main spines. *Sepsagon* also has one longer and two shorter spines but the shorter spines are equally developed. In the samples from Svilaja, *Pseudostylosphaera* is common but all specimens belong to *P. tenuis*. In samples from Monte San Giorgio, eight different species of *Pseudostylosphaera* occur (Stockar et al., 2012).

Genus ***Parasepsagon*** Dumitrica, Kozur and Mostler, 1980

Parasepsagon longobardicus (Kozur and Mostler, 1981)
Plate 2, figs. 18–20

1981 *Tiborella longobardica* n. sp. – Kozur and Mostler, 79, pl. 51, fig. 2.
1995 *Sepsagon*? *dercourti* n. sp. – Kellici and De Wever, 157, pl. 5, figs. 6 and 7.

Remarks: This species differs from *Parasepsagon praetetracanthus* Kozur and Mostler (1994, p. 49, pl. 55, fig. 3; see also Stockar et al., 2012, p. 401, pl. 5, figs. 18, ?19–20) by having spines of unequal length. It is similar to *Parasepsagon longidentatus* (Kozur and Mostler) (1981, 71, pl. 51, fig. 1; see also Stockar et al., 2012, p. 401, pl. 5, fig. 15) but has a more spherical shell and proportionally thinner spines. *P. longobardicus* and *P. longidentatus* have one longer and three equal shorter spines, suggesting their close relationship with *Muelleritortis* Kozur, which is a typical Ladinian genus. *Parasepsagon longobardicus* has a scarce record in the Longobardian (Kozur and Mostler, 1981) and in the upper Illyrian–Fassanian (Kellici and De Wever, 1995).

Genus ***Bernoulliella*** Stockar, Dumitrica and Baumgartner, 2012

***Bernoulliella* sp.**
Plate 2, fig. 21

Remarks: This species is assigned to *Bernoulliella* because it has six spines and a double-layered cortical shell typical of Hindeosphaeridae. It is considerably smaller than *Bernoulliella simplex* (Lahm), which is thus far the only described species of the genus. Just one specimen was found in sample 4C-6.

Order SPUMELLARIA Ehrenberg, 1876
Family XIPHOSTYLIDAE Haeckel, 1881
Genus ***Archaeocenosphaera*** Pessagno and Yang *in* Pessagno et al., 1989

Archaeocenosphaera igoi (Sashida), *in* Sashida et al., 2000
Plate 3, fig. 11

1984 *Cenosphaera clathrata* Parona – Lahm, p. 15, pl. 1, figs. 1–2.
1984 *Cenosphaera* sp. B – Lahm, p. 16, pl. 1, figs. 5–6.
2000 *Cenosphaera igoi* n. sp. – Sashida et al., p. 804, Figs. 10.7–10.8.
2012 *Archaeocenosphaera* sp. B – Stockar et al., p. 409, pl. 7, figs. 10–11.
2023 *Archaeocenosphaera igoi* (Sashida) – Ozsvárt et al., p. 25, pl. 5, figs. 1–2 (and the synonymy therein).

***Archaeocenosphaera* sp. C** *sensu* Lahm, 1984
Plate 3, fig. 12

1984 *Cenosphaera* sp. C – Lahm, p. 16, pl. 1, figs. 7–8.

Remarks: In comparison with *Archaeocenosphaera igoi* (Sashida), this species is considerably larger and has a finer meshwork of more numerous small pores.

Family INTERMEDIELLIDAE Lahm, 1984
Genus ***Paurinella*** Kozur and Mostler, 1981

Paurinella mesotriassica Kozur and Mostler, 1981
Plate 3, fig. 1

1981 *Paurinella mesotriassica* n. sp. – Kozur and Mostler, p. 50, pl. 44, figs. 1a–c.
1984 *Paurinella mesotriassica* Kozur and Mostler – Lahm, p. 50, pl. 8, fig. 6.

Remarks: This specimen is assigned to *Paurinella mesotriassica* even though it lacks tiny by-spines, which Kozur and Mostler (1981) defined as a characteristic feature of this species. Such tiny spines can easily be lost due to preservation. We consider that the main difference between *P. mesotriassica* and its closely related species *P. aequispinosa* Kozur and Mostler (1981, p. 50, pl. 42, fig. 1a, b, pl. 43, fig. 1) is the shape of the main spines. In *P. mesotriassica*, the main spines are thinner and not widened in the middle part.

Genus ***Triassospongosphaera*** Kozur and Mostler, 1981

Triassospongosphaera multispinosa (Kozur and Mostler, 1979)
Plate 3, fig. 4

1979 *Acanthosphaera*? *multispinosa* n. sp. – Kozur and Mostler, p. 50, pl. 20, fig. 3.
1981 *Triassospongosphaera multispinosa* (Kozur and Mostler) – Kozur and Mostler, p. 67, pl. 58, fig. 3.
2012 *Triassospongosphaera multispinosa* (Kozur and Mostler) – Stockar et al., p. 412, pl. 8, figs. 10–11.
2023 *Triassospongosphaera multispinosa* (Kozur and Mostler) – Ozsvárt et al., p. 27, pl. 6, figs. 2–3 (and the synonymy therein).

***Triassospongosphaera*? spp.**
Plate 3, figs. 2, 3

Remarks: Specimens of this group have a large cortical shell with a spongy outer layer and long spines that are circular in cross section

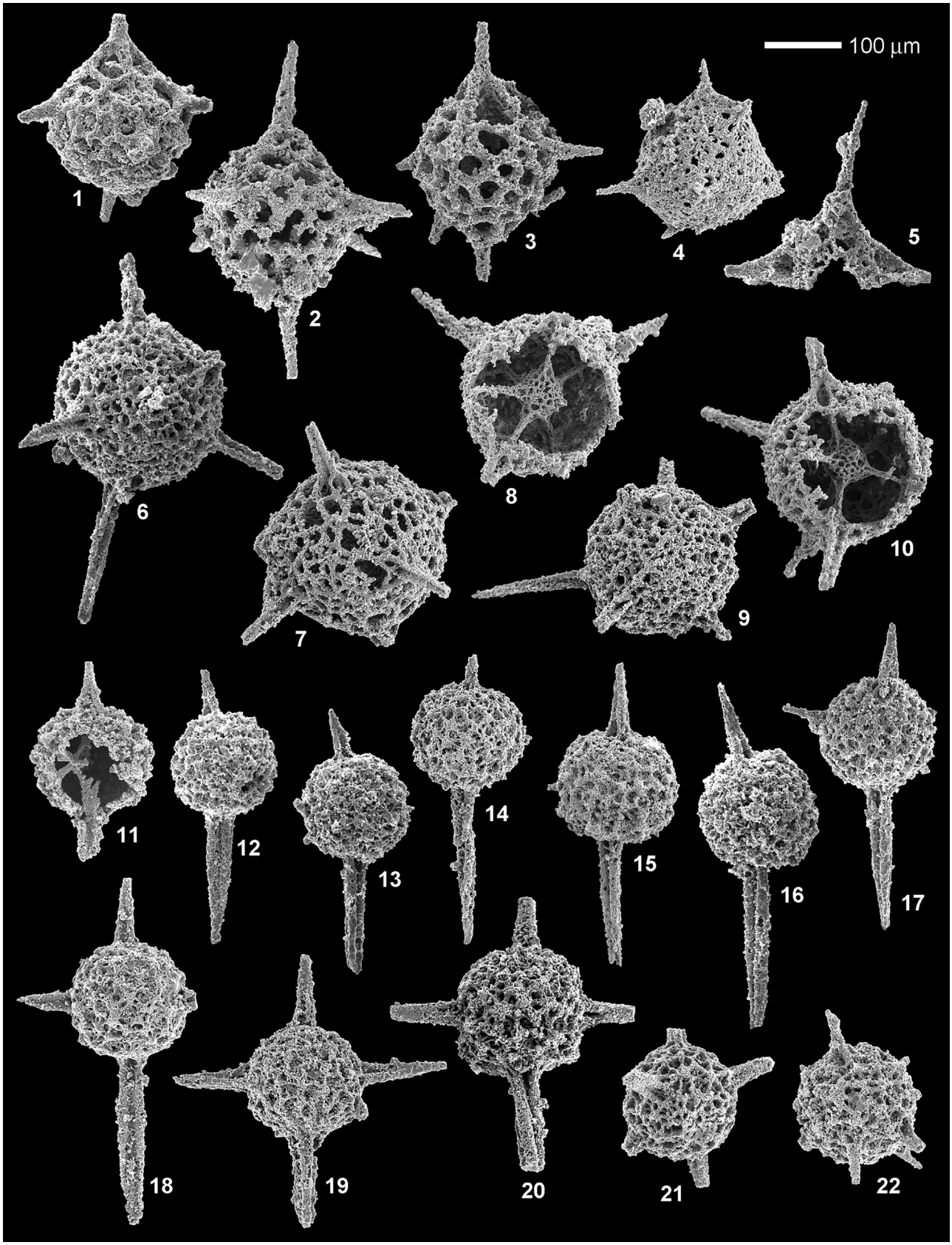

Plate 2. 1–3. *Pentactinocarpus tetracanthus* Dumitrica. 4. *Pentactinocapsa quadripes* Dumitrica. 5. *Tiborella* sp. 6–10. *Parentactinosphaera* cf. *fassanensis* (Kozur and Mostler). 11–17. *Pseudostylosphaera tenuis* (Nakaseko and Nishimura). 18–20. *Parasepsagon longobardicus* (Kozur and Mostler). 21. *Bernoulliella* sp. 22. *Thaisphaera minuta* Sashida and Igo. figs. 1–10, 12–17, 19 – sample 3C-6; figs. 11, 18, 20–22 – sample 4C-6. Scale bar 100 µm for all figures.

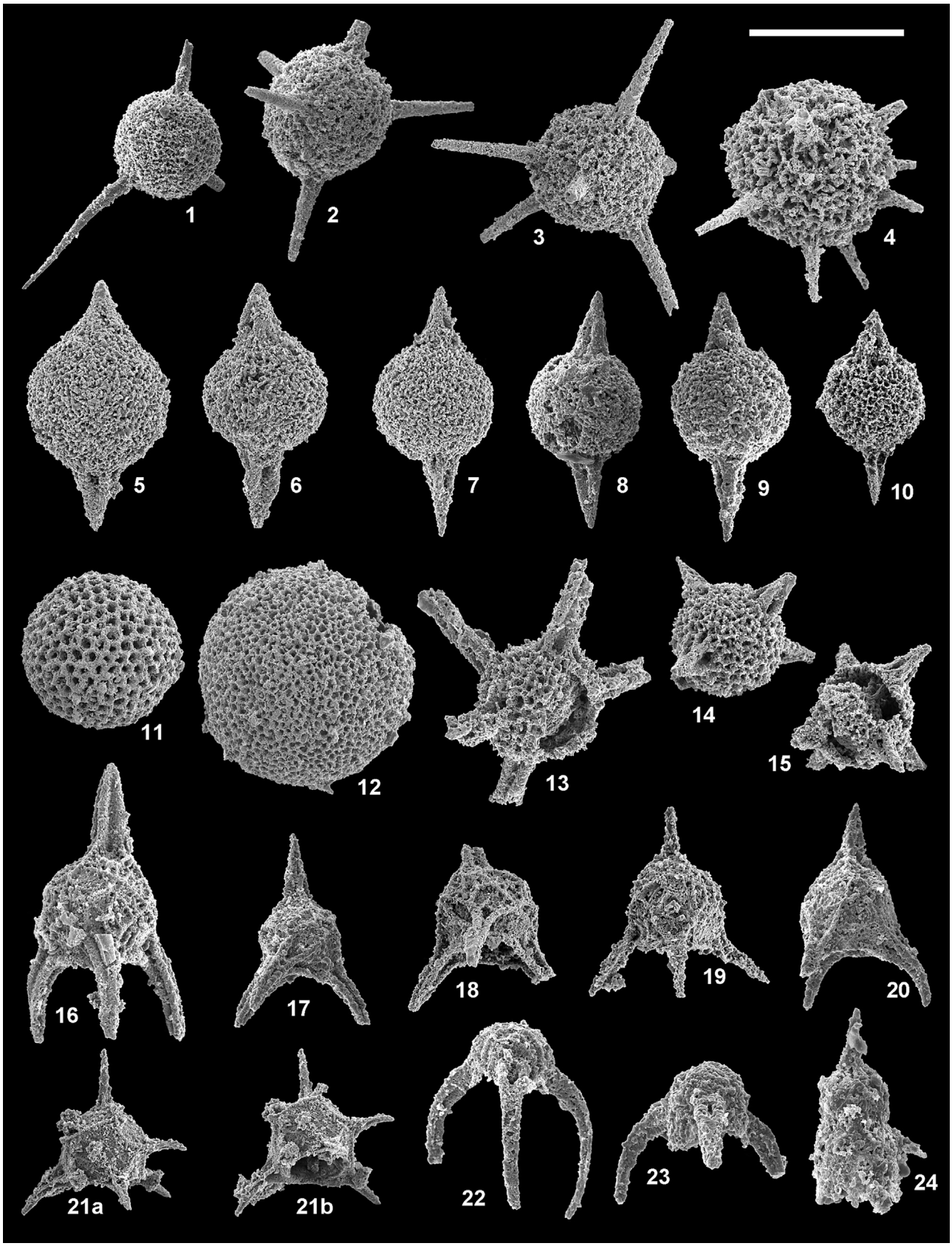

Plate 3. 1. *Paurinella mesotriassica* Kozur and Mostler. 2–3. *Triassospongosphaera*? spp. 4. *Triassospongosphaera multispinosa* (Kozur and Mostler). 5–10. *Spongopallium* aff. *koppi* (Lahm) *sensu* Tekin and Sönmez (2010). 11. *Archaeocenosphaera igoi* (Sashida). 12. *Archaeocenosphaera* sp. C *sensu* Lahm (1984). 13. "*Entactinosphaera*" cf. *simoni* Kozur and Mostler. 14–15. *Pessagnollum*? aff. *hexaspinosum* Stockar, Dumitrica and Baumgartner. 16–20. *Hozmadia reticulata* Dumitrica, Kozur and Mostler. 21a–b. *Neopylentonema* sp. A. 22. *Poulpus curvispinus* Dumitrica, Kozur and Mostler. 23. *Poulpus oertlii* (Kozur and Mostler). 24. *Pyramicyrtium*? sp. figs. 1–9, 11–13, 17–24 – sample 3C-6; figs. 10, 14–16 – sample 4C-6. Scale bar 300 μm for figs. 1–3, 200 μm for figs. 4–13, 150 μm for figs. 14–23, 100 μm for fig. 24.

through most of their length. The number of spines varies but is always more than four and less than in typical *Triassospongosphaera* species (14 in *T. triassica* (Kozur and Mostler), >20 in *T. multispinosa* (Kozur and Mostler)). Several species may be included.

Family SPONGOPALLIIDAE Kozur, Krainer and Mostler, 1996
Genus ***Spongopallium*** Dumitrica, Kozur and Mostler, 1980

Spongopallium* aff. *koppi (Lahm, 1984) *sensu* Tekin and Sönmez, 2010
Plate 3, figs. 5–10
aff. 1984 *Cromyostylus*? *koppi* n. sp. – Lahm, p. 68, pl. 12, figs. 1–2.
2010 *Spongostylus* aff. *koppi* (Lahm) – Tekin and Sönmez, p. 208, Text-fig. 6E.
2012 *Spongopallium* sp. aff. *S. koppi* (Lahm) *sensu* Tekin and Sönmez, 2010 – Stockar et al., p. 416, pl. 9, fig. 4.
? 2023 *Spongopallium* sp. – Kukoč et al., fig. 6-ag.

Remarks: This species differs from *Spongopallium koppi* by having considerably shorter spines. It further differs from *Spongopallium contortum* Dumitrica, Kozur and Mostler (1980, p. 16, pl. 2, fig. 5; pl. 11, fig. 1) in that the spines are pyramidal with a wide base. In some specimens, short secondary grooves are developed at the base of spines (pl. 3, figs. 5, 7, 8).

SPUMELLARIA INCERTAE SEDIS
Genus ***Thaisphaera*** Sashida and Igo, 1992

Thaisphaera minuta Sashida and Igo, 1992
Plate 2, fig. 22

1992 *Thaisphaera minuta* n. sp. – Sashida and Igo, p. 1306, fig. 4.8, 4.11–14, 4.16, 4.17.
2012 *Thaisphaera*? sp. cf. *T. minuta* Sashida and Igo – Stockar et al., p. 422, pl. 10, figs. 13–15.

Remarks: The structure of the cortical shell as well as the structure and distribution of spines, and the overall size of the illustrated specimen, accord well with *Thaisphaera minuta* Sashida and Igo. Only one specimen was found in sample 4C-6; its inner structure was not observed.

Genus ***Pessagnollum*** Kozur, Krainer and Mostler, 1996

Pessagnollum*? aff. *hexaspinosum Stockar, Dumitrica and Baumgartner, 2012
Plate 3, figs. 14–15

aff. 2012 *Pessagnollum*? *hexaspinosum* n. sp. – Stockar et al., p. 423, pl. 10, figs. 16–19.

Remarks: This species has much smaller pores and more robust spines than *Pessagnollum*? *hexaspinosum.* Only two specimens were found.

ENTACTINARIA OR SPUMELLARIA INCERTAE SEDIS
"***Entactinosphaera*" cf. *simoni*** Kozur and Mostler, 1979
Plate 3, fig. 13

cf. 1979 *Entactinosphaera*? *simoni* n. sp. – Kozur and Mostler, p. 70, pl. 4, fig. 5, pl. 7, fig. 2, pl. 8, fig. 1.
cf. 1984 *Entactinosphaera*? *simoni* Kozur and Mostler – Lahm, p. 17, pl. 1, fig. 10.

Remarks: With its spherical latticed cortical shell and probably six stout primary spines, this incomplete specimen is the most similar to *Entactinosphaera*? *simoni* as illustrated by Kozur and Mostler (1979) and Lahm (1984) (see the synonymy). The genus name *Entactinosphaera* was erroneously used for Mesozoic occurrences (see remarks under "*Entactinosphaera*"? cf. *triassica* Kozur and Mostler and "*Entactinosphaera*"? *zapfei* Kozur and Mostler in Stockar et al., 2012), but a correct assignment of Triassic *Entactinosphaera* species to another genus has yet to be proposed and cannot be clarified in our material due to the poor preservation.

Order NASSELLARIA Ehrenberg, 1876
Family POULPIDAE De Wever, 1981
Genus ***Poulpus*** De Wever *in* De Wever et al., 1979

Poulpus curvispinus Dumitrica, Kozur and Mostler, 1980
Plate 3, fig. 22

1980 *Poulpus curvispinus* n. sp. – Dumitrica et al., p. 22, pl. 2, fig. 1; pl. 15, figs. 5, 6.
1994 *Poulpus curvispinus praecurvispinus* n. subsp. – Kozur and Mostler, p. 116, pl. 32, figs. 3, 6, 7.
2012 *Poulpus curvispinus* Dumitrica, Kozur and Mostler – Stockar et al., p. 429, pl. 12, figs. 4–5 (and the synonymy therein)
2023 *Poulpus curvispinus praecurvispinus* Kozur and Mostler – Ozsvárt et al., p. 40, pl. 13, figs. 4–5.

Poulpus oertlii (Kozur and Mostler, 1979)
Plate 3, fig. 23

1979 *Parapoulpus oertlii* n. sp. – Kozur and Mostler, p. 88, pl. 7, fig. 5.
1981 *Parapoulpus oertlii* (Kozur and Mostler) – Kozur and Mostler, p. 81, figs. 2a–c.
2017 *Poulpus oertlii* (Kozur and Mostler) – Ozsvárt et al., p. 145, pl. 2, fig. 3.

Remarks: The illustrated specimen is assigned to *P. oertlii* (Kozur and Mostler) because it bears a short velum. Alternatively, it could be assigned to *P. curvispinus* if the velum (considered thorax in some publications) is not regarded as diagnostic. Such intraspecific variability including specimens with and without a velum was well demonstrated for *Poulpus piabyx* De Wever in a very well-preserved Carnian assemblage from Turkey (Ozsvárt et al., 2017). Generally, specimens with a velum are very rare and this is the first record of *P. oertlii* in the Ladinian. All previously reported *P. oertlii* (see the synonymy) are Carnian in age.

Genus ***Hozmadia*** Dumitrica, Kozur and Mostler, 1980

Hozmadia reticulata Dumitrica, Kozur and Mostler, 1980
Plate 3, figs. 16–20

1980 *Hozmadia reticulata* n. sp. – Dumitrica et al., p. 21, pl. 9, figs. 9–10.
1994 *Hozmadia costata* n. sp. – Kozur and Mostler p. 114, pl. 31, figs. 1, 2, 5–10.
1995 *Hozmadia reticulata* Dumitrica, Kozur and Mostler – Ramovš and Goričan, p. 186, pl. 7, figs. 1–4 (and the synonymy therein).
1995 *Hozmadia reticulata* Dumitrica, Kozur and Mostler – Kellici and De Wever, p. 148, pl. 2, figs. 17, 18.
1995 *Hozmadia costata* Kozur and Mostler – Kellici and De Wever, p. 148, pl. 2, figs. 15–16; pl. 4, figs. 20–21.
? 2012 *Hozmadia* cf. *reticulata* Dumitrica, Kozur and Mostler – Stockar et al., p. 429, pl. 12, fig. 6.
2023 *Hozmadia costata* Kozur and Mostler – Ozsvárt et al., p. 40, pl. 13, figs. 6–7 (and the synonymy therein).
2023 *Hozmadia reticulata* Dumitrica, Kozur and Mostler – Ozsvárt et al., p. 41, pl. 13, figs. 8–9 (and the synonymy therein).

Remarks: Hozmadia costata Kozur and Mostler is considered a synonym of *H. reticulata*. By definition, *H. costata* has a smooth and *H. reticulata* a reticulate surface between the ridges but transitional morphotypes usually co-exist (see the synonymy, e.g., Kellici and De Wever, 1995). No difference in stratigraphic range of the two species has been demonstrated implying that a more or less developed ornamentation could be related to the ontogenetic stage or some environmental factors. *H. retic-*

ulata is the only nassellarian species, which is relatively abundant in the studied samples.

Genus ***Neopylentonema*** Kozur, 1984

***Neopylentonema* sp. A**
Plate 3, figs. 21a, b

Remarks: This species differs from all other species of *Neopylentonema* by having simple carinate spines without branches. Only one specimen was found.

Family ANISICYRTIDAE Kozur and Mostler, 1981

Genus ***Pyramicyrtium*** Dumitrica, 2017
Type species: *Pyramicyrtium pyramidale* Dumitrica, 2017

***Pyramicyrtium*? sp.**
Plate 3, fig. 24

Remarks: This poorly preserved dicyrtid is the only nassellarian with more than one segment that we found in the samples from Mt. Svilaja. Based on its size, general outline, and the orientation of spines, we questionably assign it to *Pyramicyrtium*.

7. Discussion

7.1. Depositional environment

The succession of various rock types ranging from tuffs, cherts, limestones, and dolostones was deposited in a specific deeper-marine environment. The presence of vitriclastic tuffs, comprising bubble-wall shards, signifies the influence of explosive (volatile rich) volcanism during dominantly carbonate sedimentation. The volcanic eruption probably occurred in the relative vicinity of the depositional realm in shallow-water environment or even on land but pyroclastic material was likely deposited in a deeper/pelagic basinal environment by different gravitational mechanisms including pyroclastic density currents as mentioned for similar deposits by Di Capua and Groppelli (2016, 2018) and Di Capua et al. (2023) that show some similarities to turbidites in the siliciclastic sense (Carey and Schneider, 2011). Chert beds with preserved radiolarians signify deeper pelagic environmental conditions. The preservation of radiolarians can be correlated with the increase of silica content in the environment due to volcanism. The presence of thin-shelled bivalves usually confirms deeper/pelagic conditions, also supported by the presence of ammonoids and fragments of crinoids. The presence of grainy limestone types can be explained by limy detritus resedimented from the shallower parts of the environment. In the Middle Triassic deposits of the Dinarides, resedimentation from limestone-dominated structurally higher blocks to the deep-water basins was common (Balini et al., 2006; Celarc et al., 2013; Smirčić et al., 2018, 2024). Clasts of carbonate rocks are interpreted as lithoclasts derived from moderately or completely lithified shallow-water carbonate rocks. The rare presence of algae and benthic foraminifera (see also Chorowicz and Termier, 1975) confirms their primary origin in shallow waters of the tectonically elevated blocks, as well. Subsequent mixing with pelagic detritus (radiolarians, thin-shell bivalves, crinoids, ammonoids) indicates resedimentation and the incorporation of bioclasts during transport. The mechanism of resedimentation included high-density currents as suggested by the thick breccia bed near the top of the studied section. Large fragments of land plants (e.g., *Equisetites*, Fig. 4c) indicate the vicinity of land likely present on the tectonically elevated blocks.

The macrocrystalline dolostone texture has characteristics of the late diagenetic dolomitization phase. Dolostones are usually severely silicified and apparently related to the specific conditions where dolomitization and silicification occur together as diagenetic processes. Silica deposited as nodules or along bedding planes originated from dissolved radiolarian tests and from the increased silica content in a marine environment due to the dissolution of pyroclastic material. The formation of dolomite could be related to the presence of organic matter as organic matter decomposition through bacterial sulphate reduction increases pore water alkalinity and promotes the precipitation of dolomite. Such an explanation was, for example, proposed for Middle Triassic organic matter-rich dolomites of the Southern Alps (Bernasconi, 1994; Meister et al., 2013). Dolomitization may have occurred coevally with the later stage of silica transformation. As demonstrated by experimental studies, the transformation of opal-A (amorphous silica) to opal-CT (disordered cristobalite and tridymite) inhibits dolomitization, but the subsequent transformation of opal-CT to quartz favors the formation of dolomite (Baker and Kastner, 1981).

Brachiopods and bivalves are characterized by small-sized specimens and low diversity, as first described by Chorowicz and Termier (1975) who concluded that they represent the epifauna of algal meadows in a very shallow and isolated marine environment. Halamski et al. (2015) confirmed the low diversity and high degree of endemism for brachiopods (all of them are very small, only mm-sized) and likewise interpreted this assemblage as representing an ecosystem of a dasycladalean submarine meadow. Since dasycladaleans grow in shallow waters only down to 10–12 m (e.g., Piros and Preto, 2008), it is clear that this benthic community does not occur in situ but must have been imported to the basin from a nearby carbonate shelf.

Ammonoids, which were found close to the level with brachiopods and radiolarians (Fig. 3) are also endemic. Three new species were described, one of them even ascribed to a new genus (Balini et al., 2006). Ammonoid genera, typical of open-marine deep-water environments are missing. Instead, the genus *Detoniceras*, which is known only from carbonate-platform related faunas, occurs.

Organic carbon content is low, TOC values are mostly below 0.5%, but the presence of organic matter is detected in all dark-grey limestones of the investigated section (Table 1). The preservation of organic matter indicates low oxygen content in bottom waters that may have been related to a stratified water column and poor open-marine connections in a restricted intra-platform basin. The high thermal alteration indicated by the color of the conodonts (CAI = 5.0 to 5.5 *sensu* Epstein et al., 1977) as well as by vitrinite reflectance, thermal alteration index, and maximum temperature of the pyrolysis (%R_o 1.28 to 1.52, TAI 3 to 3^+, T_{max} >460^{0}C, respectively; Table 1) and prevailing amorphous kerogen (Fig. 7) make it difficult to accurately determine the origin of organic matter. However, the remains of terrestrial plants (Fig. 4; Kerner, 1907) and presence of vitrinite particles (Fig. 7) suggest that a certain proportion of organic matter must have originated from vegetation on the emerged land (kerogen type III).

The intra-platform restricted-basin setting was proposed for the Svilaja section in previous research (Belak, 2000; Smirčić et al., 2018). Here, we recall that the entire 150-m-thick succession of deeper-water siliceous carbonates (Fig. 2) is characteristically dark-grey to black, indicating oxygen-deficient environmental conditions through the entire section and suggesting that the basin configuration with limited connectivity to the open sea was established during the initial subsidence pulse in the Late Anisian and persisted until the end of the pelagic episode in the latest Ladinian–Early Carnian. A system of semi-enclosed intra-platform basins, extending from northern Croatia (Smirčić et al., 2020) to northern Albania (Gaetani et al., 2015), was formed on the High Karst structural high but individual semi-enclosed basins may have also developed on smaller topographic highs of the rifted continental margin.

During the Middle Triassic, the Dinarides were placed at a northern intertropical latitude of 10–20° (Schettino and Turco, 2011). The climate was governed by a strong global monsoon with seasonal rainfall, concentrated during the summer in the northern hemisphere (Parrish, 1993; a review in Preto et al., 2010). Based on multidisciplinary research of carbonate platforms in the Dolomites, Stefani et al. (2010) constructed

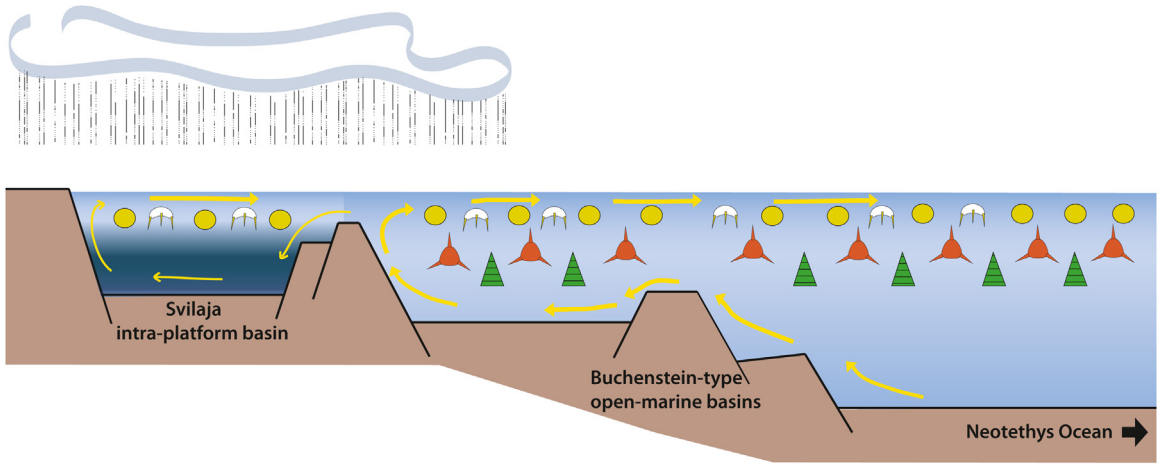

Fig. 9. Circulation model for the latest Anisian–Early Ladinian comparing semi-enclosed intra-platform basins (like the Svilaja basin) with open marine Buchenstein type basins of the Adria continental margin. In the restricted basins, the input of fresh water from the continent caused the stratification of water masses and generated oxygen-depleted, possibly euxinic conditions in which only surface-dwelling radiolarians could survive. Conversely, the Buchenstein type basins, eventually separated from the ocean by lower-lying sills, were better connected with the open sea, fully oxygenated and populated by the entire spectrum of radiolarian taxa living in the ocean (yellow arrows are for water currents, different shapes and colors of radiolarians for their depth preferences).

a climate framework that could also be valid in the Dinarides because these areas are geographically close and were located in approximately the same paleolatitude. According to these authors, the Triassic climate was generally dry and warm with five pulses toward a moister climate, among them one in the Middle Anisian and the next one in the Late Ladinian; the Late Anisian to Early Ladinian interval was predominantly dry. From the presence of terrestrial plant debris including the horsetail *Equisetites*, which requires a humid environment (Pott et al., 2008) and also occurs in all Triassic plant localities of the Southern Alps (Kustatscher et al., 2019), we infer that even during the Late Anisian–Early Ladinian interval the precipitation and fresh-water influx to the intra-platform basins were sufficient to surpass the evaporation. The excess fresh water promoted stratification of the water column and allowed for an estuarine circulation with a flow of lighter low-salinity surface water from the restricted basin to the open sea and the incursion of saline bottom waters in the opposite direction (Fig. 9). The likely primary cause of the oxygen deficiency in the intra-platform basin was the poor vertical mixing of water masses. The lower part of the water column may have been euxinic, poisoned with hydrogen sulphide and uninhabitable.

7.2. Comparison with radiolarian assemblages from other sites

Common radiolarians in the low-diversity assemblage from the Svilaja section are Pentactinocarpidae, Hindeosphaeridae (mostly *Pseudostylosphaera*), *Parentactinosphaera, Spongopallium* and *Hozmadia* (Table 4). Among Pentactinocarpidae, *Lobactinocapsa* with a thickened spongy cortical shell (Pl. 1) is abundant. The most apparent peculiarity of this assemblage is the absence of multicyrtid nassellarians, Eptingiidae and Oertlispongidae. Multicyrtid nassellarians (e.g., *Triassocampe, Pararuesticyrtium*), *Eptingium*, and detached spines of Oertlispongidae are robust dissolution-resistant morphotypes that are systematically found even in poorly preserved and incomplete material from cherts associated with ophiolites (e.g., Dumitrica and Mello, 1982; Gawlick et al., 2008; Goričan et al., 2022; Kukoč et al., 2024). The absence of these taxa is thus considered to relate to the primary composition of thanatocoenoses. We rule out a major preservation bias also because many specimens still retain their fragile inner structure (Pls. 1, 2).

The Svilaja radiolarian assemblage is the most similar to the Early Ladinian fauna of the San Giorgio Dolomite, for which the inferred depositional environment is also an intra-platform basin with dysoxic to anoxic bottom water conditions (Stockar et al., 2012). A comparison of distribution of genera and their qualitative abundance estimates reveal some major similarities but also differences between these two faunas (Table 4). Pentactinocarpidae, Heptacladidae, and Hindeosphaeridae are characteristically common in both assemblages. The most obvious common trait differentiating these two faunas from "normal" high-diversity faunas of the Buchenstein and equivalent formations (e.g., Ozsvárt et al., 2023; see Fig. 1 for localities and the list of references) is the small number of nassellarians, particularly the almost complete absence of multicyrtids. Nevertheless, the assemblage from Svilaja containing 19 genera is even more impoverished than that from Monte San Giorgio with 42 genera. It is devoid of Eptingiidae, Oertlispongidae, and Relindellidae. *Triassothamnus* is also missing, but considering its delicate skeleton this absence could be related to diagenetic not ecological factors. A significant difference between the two faunas is the abundance of sponge spicules. They are abundant in all samples from Monte San Giorgio but extremely rare on Mt. Svilaja. These observations imply a higher degree of environmental stress and probably more expanded hypoxia in the Svilaja basin.

In modern oceans, different radiolarian species occupy different depth intervals; in addition to species living near the surface, many species live exclusively in deeper water (Casey et al., 1979; Itaki, 2003; Boltovskoy et al., 2017). The depositional depth for the radiolarian-bearing horizon on Mt. Svilaja can be estimated at roughly 100 m if we consider its position 50 m below the emersion breccia (Fig. 2) and a compaction coefficient 0.5 (Schmoker and Halley, 1982) as an average value for limestones. Similar estimations of a relatively shallow depth varying between 30 m and 100 m were obtained for the Monte San Giorgio basin (Bernasconi, 1994). Likewise, the majority of highly diversified Middle Triassic radiolarian assemblages from the western Tethys were reported from sediments of relatively shallow basins. The Buchenstein Formation, which contains the best-known high-diversity faunas, represents only a short pelagic episode within a succession of platform carbonates; its depositional depth may have been as shallow as 200–250 m (Berra and Carminati, 2010). The continental-margin Buchenstein-type sites in the Dinarides (Fig. 1) are also overlain by platform limestone and were deposited in water depths not exceeding a few hundred meters (Goričan et al., 2005; Gawlick et al., 2012; Kukoč et al., 2023). Thus, the relatively shallow water depth cannot be the main reason for the specific composition of the assemblage from Mt. Svilaja. It is more likely that

Table 4
Distribution and abundance of radiolarian genera at Mt. San Giorgio (Stockar et al., 2012) and at Mt. Svilaja (this study).

Order / Family / Genus	FAD	Mt. San Giorgio	Mt. Svilaja
Order Entactinaria			
Pentactinocarpidae			
Pentactinocarpus	Late Anisian	A	R
Pentactinocapsa	Mid. Anisian	/	R
Lobactinocapsa	Late Anisian	/	A
Thalassothamnidae			
Triassothamnus	Mid. Anisian	A	/
Eptingiidae			
Eptingium	Early Anisian	A	/
Pylostephanidium	Late Anisian	R	/
Multiarcusellidae			
Tiborella	L. Olenekian	R	R
Heptacladidae			
Heptacladus	Mid. Anisian	C	/
Parentactinosphaera	Mid. Anisian	R	C
Hindeosphaeridae			
Pseudostylosphaera	L. Olenekian	A	C
Parasepsagon	Mid. Anisian	C	R
Sepsagon	Mid. Anisian	C	/
Bernoulliella	Mid. Anisian	A	R
Entactinaria incertae sedis			
Hexatortilisphaera	Mid. Anisian	R	/
Eohexastylus	Mid. Anisian	C	/
Order Spumellaria			
Xiphostylidae			
Archaeocenosphaera	Mid. Anisian	A	R
Novamuria	Late Anisian	A	/
Intermediellidae			
Paurinella	Late Permian	R	R
Angulopaurinella	Late Anisian	R	/
Triassospongosphaera	Late Anisian	A	R
Astrocentrus	Mid. Anisian	R	/
Plafkerium	Mid. Anisian	R	/
Relindellidae			
Pentaspongodiscus	Mid. Anisian	C	/
Relindella	Mid. Anisian	C	/
Spongopalliidae			
Spongopallium	Mid. Anisian	R	C
Oertlispongidae			
Pararchaeospongoprunum	Late Permian	C	/
Paroertlispongus	Mid. Anisian	C	/
Oertlispongus	Late Anisian	A	/
Baumgartneria	Late Anisian	A	/
Falcispongus	Late Anisian	R	/
Flexispongus	Late Anisian	R	/
Pseudohagiastridae			
Acanthotetrapaurinella	Ladinian	R	/
Cantalum?	Early Norian	R	/
Spumellaria incertae sedis			
Thaisphaera	Late Induan	C	R
Pessagnolum?	Mid. Anisian	R	R
Carinaheliosoma?	E. Carnian	R	/
Ticinosphaera	Late Anisian	A	/
Lahmosphaera	Late Anisian	A	/
Entactinaria or Spumellaria incertae sedis			
"*Entactinosphaera*"		R	R
Order Nassellaria			
Poulpidae			
Poulpus	Late Anisian	R	R
Hozmadia	L. Olenekian	R	C
Eonapora?	Mid. Anisian	R	/
Neopylentonema	Mid. Anisian	/	R
Ultranaporidae			
Silicarmiger	Mid. Anisian	R	/
Anisicyrtidae			
Pyramicyrtium?	L. Olenekian	/	R
Ruesticyrtidae			
Pararuesticyrtium?	Mid. Anisian	R	/
sponge spicules		A	R

Abbreviations: / not present; *R* rare; C common; *A* abundant (applied if at least one species of the genus is abundant). First appearance datums (FADs) in the second column according to O'Dogherty et al. (2009).

such impoverished assemblages are characteristic of restricted oxygen-deficient basins, as was also inferred for the Monte San Giorgio basin (Stockar et al., 2012).

Modern radiolarians show the highest diversity in open-ocean environments with normal salinity whereas near-shore areas are characterized by lower diversity and the predominance of very few species (e.g., Casey, 1993; Boltovskoy et al., 2017). Many inner and marginal seas, for example the Black Sea, are devoid of radiolarians but radiolarians can be common in marginal seas intruded by oceanic waters, as with the case of Norwegian fjords (Boltovskoy et al., 2017). The fjords are characterized by seasonal fresh-water input, estuarine circulation, and a stratified water column; their radiolarian diversity is low and, due to the restricted water exchange, the population structure varies geographically between fjords and even within the same fjord (Swanberg and Bjørklund, 1986, 1987). The environmental conditions in the fjords could be analogous to those in the Middle Triassic Svilaja basin but a more detailed comparison of radiolarian faunas is hampered by the fact that fossil and living species are not directly related. Further, Norway is located at high latitudes, whereas the paleolatitude of the Svilaja basin was in the intertropical belt. Nonetheless, we note that among the major nassellarian species in the fjords there is only one multi-segmented species: *Stichocorys seriata* Jørgensen. This species is relatively rare in the main fjords and completely absent from their smaller branches, the polls, which are more isolated and anaerobic at depth; these polls exhibit specific low-diversity faunas dominated by one or two species only (Swanberg and Bjørklund, 1987). Interestingly, these species belong to dicyrtid (*Amphimelissa, Lithomelissa*) or spicular (*Plagiacantha*) nassellarians.

In the present-day oceans in general, most multicyrtid nassellarians are encountered in deeper waters (Casey et al., 1979) and a similar distribution can be inferred from the Mesozoic record. For example, in low-latitude Upper Cretaceous material there is also a marked increase in the abundance of multicyrtid nassellarians in deep-water faunas (Empson-Morin, 1984). This distribution could suggest that in the oxygen-deficient Svilaja and Monte San Giorgio basins the deep-dwelling species were brought to the basin from the open sea and then eliminated due to lethal conditions in the lower water column. An alternative explanation would be that the deep-water species could not reach the marginal basin because the sill was too shallow. Such an explanation was proposed for the present-day Japan Sea, which lacks deep-water species of the adjacent northwestern Pacific (Itaki, 2003). We prefer the first interpretation given that significant differences exist between the Japan Sea and the Svilaja basin. The Japan Sea is much larger and considerably deeper, up to 3 700 m, with radiolarians living down to 2000 m depth; the deep-water is cold and well oxygenated, and characterized by its proper circulation independent of that of the open oceans (Itaki, 2003).

The majority (but not all) multicyrtid nassellarians in modern seas prefer deep water and we may assume that some Triassic multicyrtids may also have lived in shallow water. Research on laboratory cultured radiolarians showed a clear correspondence between the morphology of radiolarian skeletons and feeding mechanisms (Matsuoka, 2007). Four types of feeding behavior were recognized by Matsuoka (2007). Multicyrtid nassellarians are the most demanding and capture relatively large prey. Some other nassellarians and solitary spumellarians collect tiny prey and may bear symbiotic algae as well. The fourth group is colonial radiolarians that can live exclusively on symbiotic algae but this group is not known from the Mesozoic. We could speculate that the stratification in the Svilaja basin prevented upwelling and caused nutrient starvation that was most unfavorable for multicyrtid nassellarians. Still, since ammonoids and conodont animals at the top of the food chain lived successfully in this basin it is unlikely that the potentially low productivity was the major stressor affecting radiolarians.

The decline of deep-water radiolarians in direct relation to reduced oxygen levels is well documented for the Paleozoic. As a response to the expansion of oceanic anoxia on a global scale, typical deep-water order Albaillellaria disappeared almost completely already during the

initial stage of the stepwise extinction at the Permian–Triassic transition whereas shallow-water spherical radiolarians resisted much longer (Feng and Algeo, 2014). More specifically, Shi et al. (2016) reported on Middle Permian radiolarians from the Gufeng Formation in the northern marginal basin of the Yangtze Platform. The lower unit of this formation, deposited in oxic conditions, is dominated by albaillellarians that account for 80% of the radiolarian fauna. Conversely, the upper unit, attributed to a suboxic environment, contains exclusively spherical radiolarians. Interestingly, the disappearance of albaillellarians is concomitant with a decrease in geochemical productivity proxies and an increase in sulphur content.

It is also noteworthy that the radiolarian assemblage from Mt. Svilaja is for a large part composed of genera that thrived already in the late Early Triassic, namely, in early times of recovery after the Permian–Triassic mass extinction (De Wever et al., 2006) and towards the end of the protracted interval of permanent or episodic oceanic anoxia (Isozaki, 1997; Feng and Algeo, 2014). These genera, which newly appeared in the Spathian (Table 4), are *Tiborella, Pseudostylosphaera, Hozmadia*, and *Taisphaera* (Sugiyama, 1992; Sashida and Igo, 1992) and probably also *Parasepsagon* (see *Plafkerium*? *antiquum* in Sugiyama, 1992). Typical multicyrtid nassellarians originated later, during the early Middle Triassic (O'Dogherty et al., 2010), when fully oxygenated conditions were re-established in oceanic environments worldwide.

Fluctuations in radiolarian presence and diversity are a good proxy for the connection of marginal seas with the ocean. A fossil example applicable for comparisons with Triassic intra-platform basins is the middle Eocene Arctic basin, which was a semi-enclosed basin characterized by estuarine circulation, a low-salinity surface layer, anoxic (euxinic) conditions below the photic zone, and low oxygen concentration in the productive euphotic layer (Onodera et al., 2008). In these sediments, radiolarian assemblages occur sporadically and vary from monospecific to somewhat more diverse in relation to the more or less extensive connection to the Atlantic Ocean (Takahashi et al., 2015). In the case of the Mt. Svilaja section, we assume that the basin was permanently connected with the open sea because radiolarians occur in all samples studied. At least some very poorly preserved specimens were found in all residues of acid treatments and radiolarian ghosts are present in thin sections.

In summary, we conclude that the Svilaja basin was a semi-enclosed intra-platform basin with a strongly stratified water column, sluggish subsurface circulation, an inhabitable euphotic upper layer, and anoxic (possibly euxinic) deeper waters (Fig. 9). Radiolarians were supplied from the open sea by estuarine-type circulation, but only surface-dwelling species could prosper in this environmental setting. Most of them may have lived in symbiosis with photosynthetic organisms. Further research on sulphur, iron and redox-sensitive trace metals is needed to confirm the assumed euxinic conditions.

8. Conclusions

A moderately well-preserved Middle Triassic radiolarian assemblage of unusually low diversity was encountered in dark-colored carbonate rocks of Mount Svilaja in the External Dinarides. In total, 19 genera were identified. They belong to spherical forms of Spumellaria and Entactinaria, and to monocyrtid Nassellaria. Multicyrtid Nassellaria are absent.

Based on the associated conodonts, the radiolarian-bearing interval is assigned to the Lower Ladinian *Budurovignathus hungaricus* Zone. Facies analysis and other associated fossil remains (ammonoids, brachiopods, algae, benthic foraminifera) indicate deposition in a relatively deep marine environment with notable input from the surrounding platform areas. The organic-matter content is low but ubiquitous, and appears to have a mixed origin, incorporating both terrestrial and marine sources. Silicification and partial dolomitization are the common diagenetic features. The inferred paleogeographic setting is a semi-enclosed, oxygen-deficient intra-platform basin in the interior of the High Karst swell. This basin was formed during the Middle Anisian rifting event and was completely filled in by the latest Ladinian–Early Carnian.

The radiolarian assemblage is considerably less diverse than that of the coeval open-marine Buchenstein-type basins and is even more impoverished than the assemblage of the San Giorgio Dolomite, which was deposited in an oxygen-poor intra-platform basin and is also devoid of multicyrtid Nassellaria. The radiolarian fauna from Mt. Svilaja is to some extent comparable with the recent low-diversity faunas of Norwegian fjords, and those of ancient marginal seas, e.g., the Eocene Arctic basin, which was only sporadically connected with the open ocean. Permian examples are discussed to show a comparable lack of deep-water taxa (multicyrtid Nassellaria in the Mesozoic, Albaillellaria in the Permian) in response to expanded hypoxia. Albaillellaria are known to have locally disappeared due to reduced oxygen levels and became globally extinct at the Permian–Triassic transition due to widespread oceanic anoxia.

Considering these faunal comparisons and the generally wet climate in the Middle Triassic western Tethys, we propose a circulation model that explains the reduced radiolarian diversity in the Svilaja intra-platform basin (Fig. 9). The inflow of fresh water from the continent caused the stratification of water masses and generated oxygen-depleted, possibly euxinic conditions. The estuarine circulation supplied radiolarians from the open sea to the basin, but only shallow-water radiolarians could thrive in these environmental conditions. Although the exchange of water masses was sluggish, a permanent connection with the open ocean is inferred for the entire Middle Triassic pelagic episode.

Declaration of competing interest

The authors declare that they have no known competing financial interests or personal relationships that could have appeared to influence the work reported in this paper.

Data availability

No unpublished data were used.

Acknowledgments

This research was financially supported by the Slovenian Research and Innovation Agency (research core fundings No P1–0008 and No P1–0011) and the University of Zagreb (financial support programs 113400094, 113400112). We thank Mario Valent for preparing the thin sections, Marija Petrović for processing the conodont samples, and Murray James Bales for English language editing. We also thank Péter Ozsvárt, an anonymous reviewer, and the Editor Marie-Béatrice Forel for their critical reading and valuable comments.

References

Baker, P.A., Kastner, M., 1981. Constraints on the formation of sedimentary dolomite. Science 213, 214–216.

Balini, M., Jurkovšek, B., Kolar-Jurkovšek, T., 2006. New Ladinian ammonoids from Mt. Svilaja (External Dinarides, Croatia). Rivista Italiana di Paleontologia e Stratigrafia 112 (3), 383–395.

Bechstädt, T., Brandner, R., Mostler, H., Schmidt, K., 1978. Aborted rifting in the Triassic of the eastern and southern Alps. N. Jb. Geol. Paläont. Abh. 156 (2), 157–178.

Belak, M., Jelaska, V., Benček, Đ., Matičec, D., Belak, M., Gušić, I., 2000. Postaja 2: profil Sutina – Zelovo Sutinsko. Kristaloklastični i vitroklastični tufovi (pietra verde) s proslojcima silificiranih dolomita, vapnenca, tufita, rožnjaka. In: Geološka povijest i strukturna evolucija Vanjskih Dinarida. 2. Hrvatski Geološki Kongres. Vodić ekskurzija A-1, Zagreb, pp. 6–10 Cavtat-Dubrovnik, May 17–20, 2000.

Bernasconi, S.M., 1994. Geochemical and microbial controls on dolomite formation in anoxic environments: a case study from the Middle Triassic (Ticino, Switzerland). Contributions to Sedimentology 19, 1–109.

Berra, F., Carminati, E., 2010. Subsidence history from a backstripping analysis of the Permo-Mesozoic succession of the Central Southern Alps (northern Italy). Basin Res 22, 952–975.

Boltovskoy, D., Anderson, O.R., Correa, N.M., 2017. Radiolaria and Phaeodaria. In: Archibald, J.M., Simpson, A.G.B., Slamovits, C.H. (Eds.), Handbook of the Protists. Springer International Publishing, Berlin, pp. 731–763.

Brack, M., Nicora, A., 1998. Conodonts from the Anisian-Ladinian succession of Bagolino, Brescian Prealps (Brescia, Lombardy, Northern Italy). Giornale di Geologia Ser. 3 - 60, Spec. Issue, ECOS VII-Southern Alps Field Trip Guidebook, 314–325.

Brack, P., Rieber, H., Nicora, A., Mundil, R., 2005. The global boundary stratotype section and point (GSSP) of the Ladinian Stage (Middle Triassic) at Bagolino (Southern Alps, Northern Italy) and its implication for the Triassic time scale. Episodes 28, 233–244.

Bucković, D., Martinuš, M., 2010. Triassic terrestrial phase recorded in the carbonate platform succession of the Karst Dinarides (Croatia). Nat Croatica 19, 213–230.

Budai, T., Vörös, A., 1993. The Middle Triassic events of the Transdanubian Central Range in the frame of the Alpine evolution. Acta Geologica Hungarica 36 (1), 3–13.

Cadet, J.-P., 1978. Essai sur l'évolution alpine d'une paléomarge continentale: les confins de la Bosnie-Herzégovine et du Monténégro (Yougoslavie). Mémoires de la Société géologique de France 133, 84.

Carey, S.N., Schneider, J.L.Hüneke, H., Mulder, T. (Eds.), 2011. Volcaniclastic processes and deposition in the deep-sea. Deep-sea sediments. Develop Sedimentol 63, 457–515.

Casey, R.E., 1993. Radiolaria. In: Lipps, J.H. (Ed.), Fossil Prokaryotes and Protists. Blackwell Scientific Publications, Oxford, pp. 249–284.

Casey, R.E., Gust, L., Leavesley, A., Williams, D., Reynolds, R., Duis, T., et al., 1979. Ecological niches of radiolarians, planktonic foraminiferans and pteropods inferred from studies on living forms in the Gulf of Mexico and adjacent waters. Transact Gulf Coast Assoc Geol Soc 29, 216–223.

Celarc, B., Goričan, Š., Kolar-Jurkovšek, T., 2013. Middle Triassic carbonate-platform break-up and formation of small-scale half-grabens (Julian and Kamnik–Savinja Alps, Slovenia). Facies 59, 583–610.

Charvet, J., 1978. Essai sur un orogène alpin. Géologie des Dinarides au niveau de la transversale de Sarajevo, Publ. No. 2. Société géologique du Nord, p. 554 21 plates.

Chen, D., Luo, H., Wang, X., Xu, B., Matsuoka, A., 2019. Late Anisian radiolarian assemblages from the Yarlung-Tsangpo Suture Zone in the Jinlu area, Zedong, southern Tibet: implications for the evolution of Neotethys. Island Arc 28 (4), e12302. doi:10.1111/iar.12302.

Chen, Y., Krystyn, L., Orchard, M.J., Lai, X.L., Richoz, S., 2016. A review of the evolution, biostratigraphy, provincialism and diversity of Middle and early Late Triassic conodonts. Papers Paleontol 2 (2), 235–263. doi:10.1002/spp2.1038.

Cheng, Y.-N., 1989. Upper Paleozoic and lower Mesozoic radiolarian assemblages from the Busuanga Islands, North Palawan Block, Philippines. Bulletin Natl Museum Natur Sci 1, 129–175.

Chiari, M., Marcucci, M., Cortese, G., Ondrejickova, A., Kodra, A., 1996. Triassic radiolarian assemblages in the Rubik area, and Cukali Zone. Albania. Ofioliti 21 (1), 77–85.

Chiari, M., Bortolotti, V., Marcucci, M., Photiades, A., Principi, G., Saccani, E., 2012. Radiolarian biostratigraphy and geochemistry of the Koziakas massif ophiolites (Greece). Bulletin de la Société géologique de France 183 (4), 287–306.

Chorowicz, J., 1977. Étude géologique des Dinarides le long de la structure transversale Split-Karlovac (Yougoslavie). Villeneuve d'Ascq, Publ. No. 1. Société géologique du Nord, p. 331 (10 plates).

Chorowicz, J., Termier, G., 1975. Une faunule silicifiée nouvelle dans le Trias moyen de la Svilaja (Yougoslavie). Annales de la Société géologique du Nord 95, 231–242 pls. XX–XXI.

De Wever, P., 1981. Une nouvelle sous-famille, les Poulpinae, et quatre nouvelles espèces de *Saitoum* radiolaires mésozoïques tethysiens. Géobios 14 (1), 5–15.

De Wever, P., 1985. Sur l'existence, dès le Paléozoïque, de radiolaires siamois. Revue de Paléobiologie 4 (1), 111–116.

De Wever, P., Sanfilippo, A., Riedel, W.R., Gruber, B., 1979. Triassic radiolarians from Greece, Sicily and Turkey. Micropaleontology 25, 75–110.

De Wever, P., O'Dogherty, L., Goričan, Š., 2006. The plankton turnover at the Permo-Triassic boundary, emphasis on radiolarians. Eclogae geologicae Helvetiae 22 (Supplement 1) S49–S62.

Di Capua, A., Groppelli, G., 2016. Emplacement of pyroclastic density currents (PDCs) in a deep-sea water environment: the Val d'Aveto Formation case (Northern Apennines, Italy). J Volcanol Geotherm Res 328, 1–8.

Di Capua, A., Groppelli, G., 2018. The riddle of volcaniclastic sedimentation in ancient deep-water basin: a discussion. Sediment. Geol. 378, 52–60.

Di Capua, A., De Rosa, R., Kereszturi, G., Le Pera, E., Rosi, M., Watt, S.F.L., 2023. Volcanically derived deposits and sequences; a unified terminological scheme for application in modern and ancient environments. In: Di Capua, A., De Rosa, R., Kereszturi, G., Le Pera, E., Rosi, M., Watt, S.F.L. (Eds.), Volcanic Processes in the Sedimentary Record: When Volcanoes Meet the Environment. Special Publications 520. Geological Society, London, pp. 11–27. doi:10.1144/sp520-2021-201.

Dickson, J.A.D., 1965. A modified staining technique for carbonates in thin section. Nature 205, 587.

Djerić, N., Gawlick, H.-J., Sudar, M., 2024. The Jurassic ophiolitic mélanges in Serbia: a review and new insights. J Geol Soc London 181 (2). doi:10.1144/jgs2023-165.

Dosztály, L., Józsa, S., 1992. Geochronological evaluation of Mesozoic formations of Darnó Hill at Recsk on the basis of radiolarians and K–Ar age data. Acta Geologica Hungarica 35 (4), 371–393.

Dumitrica, P., 1978a. Family Eptingiidae n. fam., extinct Nassellaria (Radiolaria) with sagittal ring. Dari de seama ale sedintelor, Institutul de Geologie si Geofizica. Bucuresti 64, 27–38.

Dumitrica, P., 1978b. Triassic Palaeoscenidiidae and Entactiniidae from the Vicentinian Alps (Italy) and eastern Carpathians (Romania). Dari de seama ale sedintelor, Institutul de Geologie si Geofizica. Bucuresti 64, 39–54.

Dumitrica, P., 1982a. Triassic Oertlisponginae (Radiolaria) from Eastern Carpathians and Southern Alps. Dari de seama ale sedintelor. Institutul de Geologie si Geofizica 67, 57–74.

Dumitrica, P., 1982b. Foremanellinidae, a new family of Triassic Radiolaria. Dari de seama ale sedintelor. Institutul de Geologie si Geofizica 67, 75–82.

Dumitrica, P., 2013. Siamese twins and twin-like skeletons in Mesozoic Polycystine Radiolaria. Revue de micropaléontologie 56, 51–61.

Dumitrica, P., 2017. On the status of the Triassic nassellarian radiolarian family Tetraspinocyrtidae Kozur and Mostler and description of some related taxa. Revue de micropaléontologie 60, 33–85.

Dumitrica, P., Kozur, H., Mostler, H., 1980. Contribution to the radiolarian fauna of the Middle Triassic of the Southern Alps. Geologisch-Paläontologische Mitteilungen Innsbruck 10, 1–46.

Dumitrica, P., Mello, J., 1982. On the age of the Meliata Group and the Silica Nappe radiolarites (localities Držkovce and Bohúňovo, Slovak Karst, ČSSR). Geologické práce 77, 17–28.

Ehrenberg, C.G., 1839. Über die Bildung der Kreidefelsen und des Kreidemergels durch unsichtbare Organismen. Abhandlungen Der Königlichen Akademie Der Wissenschaften zu Berlin, Jahre 1838 59–147.

Ehrenberg, C.G., 1876. Fortsetzung der mikrogeologischen Studien als Gesammt-Uebersicht der mikroskopischen Paläontologie gleichartig analysirter Gebirgsarten der Erde, mit specieller Rücksicht auf den Polycystinen-Mergel von Barbados. Abhandlungen der Königlichen Akademie der Wissenschaften zu Berlin. Jahre 1875, 1–225.

Empson-Morin, K.M., 1984. Depth and latitude distribution of Radiolaria in Campanian (Late Cretaceous) tropical and subtropical oceans. Micropaleontology 30, 87–115.

Epstein, A.G., Epstein, J.B., Harris, L.D., 1977. Conodont color alteration – an index to organic metamorphism. U. S. Geol Surv Profess Paper 995, 1–27.

Espitalié, J., Deroo, G., Marquis, F., 1985. Rock Eval pyrolysis and its applications. Institut Francais du Petrole, Rueil, p. 72.

Espitalié, J., Bordenave, M.L., 1993. Rock Eval pyrolysis. In: Bordenave, M.L. (Ed.), Applied Petroleum Geochemistry. Éditions Technip, Paris, pp. 237–261.

Feng, Q., Algeo, T.J., 2014. Evolution of oceanic redox conditions during the Permo-Triassic transition: evidence from deepwater radiolarian facies. Earth-Sci Rev 137, 34–51.

Ferrière, J., Chanier, F., Baumgartner, P.O., Caridroit, M., Bout-Roumazeilles, V., Graveleau, F., et al., 2015. The evolution of the Triassic–Jurassic oceanic lithosphere: insights from the supra-ophiolitic series of Othris (continental Greece). Bulletin de la Société géologique de France 186 (6), 71–84.

Ferrière, J., Baumgartner, P.O., Chanier, F., 2016. The Maliac Ocean: the origin of the Tethyan Hellenic ophiolites. Int J Earth Sci 105, 1941–1963.

Gaetani, M., Meço, S., Rettori, R., Henderson, C.M., Tulone, A., 2015. The Permian and Triassic in the Albanian Alps. Acta Geologica Polonica 65 (3), 271–295.

Gawlick, H.-J., Frisch, W., Hoxha, L., Dumitrica, P., Krystyn, L., Lein, R., et al., 2008. Mirdita zone ophiolites and associated sediments in Albania reveal Neotethys Ocean origin. Int J Earth Sci 97, 865–881.

Gawlick, H.-J., Goričan, Š., Missoni, S., Lein, R., 2012. Late Anisian platform drowning and radiolarite deposition as a consequence of the opening of the Neotethys ocean (High Karst nappe, Montenegro). Bulletin de la Société géologique de France 183 (4), 349–358.

Gawlick, H.-J., Goričan, Š., Missoni, S., Dumitrica, P., Lein, R., Frisch, W., Hoxha, L., 2016. Middle and Upper Triassic radiolarite components from the Kcira-Dushi-Komani ophiolitic mélange and their provenance (Mirdita Zone, Albania). Revue de micropaléontologie 59, 359–380.

Gawlick, H.-J., Lein, R., Bucur, I.I., 2021. Precursor extension to final Neo-Tethys break-up: flooding events and their significance for the correlation of shallow-water and deep-marine organisms (Anisian, Eastern Alps, Austria). Int J Earth Sci 110, 419–446.

Gianolla, P., De Zanche, V., Mietto, P., 1998. Triassic sequence stratigraphy in the Southern Alps (northern Italy): definition of sequences and basin evolution. In: de Graciansky, P.C., Hardenbol, J., Jaquin, T., Vail, P.R. (Eds.), Mesozoic and Cenozoic sequence stratigraphy of European basins. SEPM Spec. Publ. Ser. 60, pp. 719–747.

Goričan, Š., Buser, S., 1990. Middle Triassic radiolarians from Slovenia (Yugoslavia). Geologija 31–32, 133–197.

Goričan, Š., Halamić, J., Grgasović, T., Kolar-Jurkovšek, T., 2005. Stratigraphic evolution of Triassic arc-backarc system in northwestern Croatia. Bulletin de la Société géologique de France 176, 3–22.

Goričan, Š., Đaković, M., Baumgartner, P.O., Gawlick, H.-J., Cifer, T., Djerić, N., et al., 2022. Mesozoic basins on the Adriatic continental margin – a cross-section through the Dinarides in Montenegro. Folia Biologica et Geologica 63 (2), 85–150.

Grgasović, T., Kolar-Jurkovšek, T., Jurkovšek, B., 2007. Preliminary report on Ladinian dasycladalean algae from Mt. Svilaja (Croatia). In: Grgasović, T., Vlahović, I. (Eds.), 9th International Symposium on Fossil Algae – Croatia 2007, Field trip guidebook and abstracts. Hrvatski geološki institut, Zagreb, p. 226.

Haas, J., Budai, T., 1999. Triassic sequence stratigraphy of the Transdanubian Range (Hungary). Geologica Carpathica 50 (6), 459–475.

Haeckel, E., 1881. Entwurf eines Radiolarien-Systems auf Grund von Studien der Challenger-Radiolarien. Jenaische Zeitschrift für Naturwissenschaft 15, 418–472.

Halamski, A.T., Bitner, M.A., Kaim, A., Kolar-Jurkovšek, T., Jurkovšek, B., 2015. Unusual brachiopod fauna from the Middle Triassic algal meadows of Mt. Svilaja (Outer Dinarides, Croatia). J Paleontol 89 (4), 553–575. doi:10.1017/jpa.2015.34.

Isozaki, Y., 1997. Permo-Triassic boundary superanoxia and stratified superocean: Records from lost deep sea. Science 276, 235–238.

Itaki, T., 2003. Depth-related radiolarian assemblage in the water-column and surface sediments of the Japan Sea. Mar Micropaleontol 47, 253–270.

Itaki, T., Bjørklund, K.R., 2008. Conjoined radiolarian skeletons (Actinommidae) from the Japan Sea sediments. Micropaleontology 53 (5), 371–389.

Jelaska, V., Kolar-Jurkovšek, T., Jurkovšek, B., Gušić, I., 2003. Triassic beds in the basement of the Adriatic-Dinaric carbonate platform of Mt. Svilaja (Croatia). Geologija 46, 225–230.

Kellici, I., De Wever, P., 1995. Radiolaires triasiques du massif de la Marmolada, Italie du nord. Revue de Micropaléontologie 38 (2), 139–167.

Kerner, F., 1907. Vorläufige Mitteilung über Funde von Triaspflanzen in der Svilaja planina. Verhandlungen der k. k. geologischen Reichanstalt 12, 294–297.

Kolar-Jurkovšek, T., 1989. New Radiolaria from the Ladinian substage (Middle Triassic) of Slovenia (NW Yugoslavia). Neues Jahrbuch für Geologie und Paläontologie. Monatshefte 1989 (3), 155–165.
Kolar-Jurkovšek, T., Jurkovšek, B., Balini, M., 2006. Conodont zonation of the Triassic basement of the Adriatic-Dinaric carbonate platform in Mt. Svilaja (External Dinarides, Croatia). In: Purnell, M.A., Donoghue, P.C.J., Aldridge, R., Repetski, J.E. (Eds.), International Conodont Symposium, 2006. Programme and abstracts, Leicester, p. 48.
Kolar-Jurkovšek, T., Jurkovšek, B., 2019. Konodonti Slovenije /Conodonts of Slovenia. Geološki zavod Slovenije / Geological Survey of Slovenia, Ljubljana, p. 265.
Kolar-Jurkovšek, T., Martínez-Pérez, C., Hrvatović, H., Aljinović, D., Goričan, Š., Skopljak, F., Jurkovšek, B., 2023. *Pseudofurnishius* (Conodonta) from the Triassic Drežnica section. Mar. Micropaleontol. 183, 102271.
Kovács, S., 1994. Conodonts of stratigraphical importance from the Anisian/Ladinian boundary interval of the Balaton Highland. Rivista Italiana di Paleontologia e Stratigrafia 99 (4), 473–514.
Kozur, H., 1972. Die Conodontengattung *Metapolygnathus* Hayashi 1968 und ihr stratigraphischer Wert. Geologisch-Paläontologische Mitteilungen Innsbruck 2 (4), 1–37.
Kozur, H., 1984. New radiolarian taxa from the Triassic and Jurassic. Geologisch-Paläontologische Mitteilungen Innsbruck 13 (2), 49–88.
Kozur, H.W., 2003. Integrated ammonoid, conodont and radiolarian zonation of the Triassic. Hallesches Jahrbuch für Geowissenschaften 25, 49–79.
Kozur, H., Mock, R., 1972. Neue Conodonten aus der Trias der Slowakei und ihre stratigraphische Bedeutung. Geologisch-Paläontologische Mitteilungen Innsbruck 2 (4), 1–20.
Kozur, H., Mostler, H., 1979. Beiträge zur Erforschung der mesozoischen Radiolarien. Teil III: die Oberfamilien Actinommacea Haeckel 1862 emend., Artiscacea Haeckel 1882, Multiarcusellacea nov. der Spumellaria und triassische Nassellaria. Geologisch-Paläontologische Mitteilungen Innsbruck 9, 1–132.
Kozur, H., Mostler, H., 1981. Beiträge zur Erforschung der mesozoischen Radiolarien. Teil IV: Thalassosphaeracea Haeckel, 1862, Hexastylacea Haeckel, 1862 emend. Petruševskaja, 1979, Sponguracea Haeckel, 1862 emend. und weitere triassische Lithocycliacea, Trematodiscacea, Actinommacea und Nassellaria. Geologisch-Paläontologische Mitteilungen Innsbruck, Sonderband 1, 1–208.
Kozur, H., Mostler, H., 1982a. Neue Conodontenarten aus dem Illyr und Fassan der Profile Fellbach und Karalm (Gailtaler Alpen, Kärnten, Österreich). Geologisch-Paläontologische Mitteilungen Innsbruck 11 (8), 291–298.
Kozur, H., Mostler, H., 1982b. Entactinaria subordo nov., a new radiolarian suborder. Geologisch-Paläontologische Mitteilungen Innsbruck 11 (12), 399–414.
Kozur, H., Mostler, H., 1983. The polyphyletic origin and the classification of the Mesozoic saturnalids (Radiolaria). Geologisch-Paläontologische Mitteilungen Innsbruck 13, 1–47.
Kozur, H., Réti, Z., 1986. The first paleontological evidence of Triassic ophiolites in Hungary. Neues Jahrbuch für Geologie und Paläontologie Monatshefte 1986 (5), 284–292.
Kozur, H., Mostler, H., 1994. Anisian to Middle Carnian radiolarian zonation and description of some stratigraphically important radiolarians. Geologisch-Paläontologische Mitteilungen Innsbruck, Sonderband 3, 39–255.
Kozur, H.W., Krainer, K., Mostler, H., 1996. Radiolarians and facies of the Middle Triassic Loibl Formation, South Alpine Karawanken Mountains (Carinthia, Austria). Geologisch-paläontologische Mitteilungen Innsbruck. Sonderband 4, 195–269.
Krystyn, L., 1983. Das Epidaurus-Profil (Griechenland) – ein Beitrag zur Conodonten–Standardzonierung des tethyalen Ladin und Unterkarn. Schriftenreihe der Erdwissenschaftlichen Kommissionen 5, 231–258.
Kukoč, D., Smirčić, D., Grgasović, T., Horvat, M., Belak, M., Japundžić, D., et al., 2023. Biostratigraphy and facies description of Middle Triassic rift-related volcano-sedimentary successions at the junction of the Southern Alps and the Dinarides (NW Croatia). Int J Earth Sci 112, 1175–1201.
Kukoč, D., Slovenec, D., Šegvić, B., Vukovski, M., Belak, M., Grgasović, T., et al., 2024. The early history of the Neotethys archived in the ophiolitic mélange of northwestern Croatia. J Geol Soc London 181 (1). doi:10.1144/jgs2023-143.
Kustatscher, E., Nowak, H., Forte, G., Roghi, G., van Konijnenburg-van Cittert, J.H.A., 2019. Triassic marco- and microfloras of the eastern Southern Alps. Geo.Alp 16, 5–43.
Lahm, B., 1984. Spumellarienfaunen (Radiolaria) aus den mitteltriassischen Buchensteiner-Schichten von Recoaro (Norditalien) und den obertriassischen Reiflingerkalken von Großreifling (Österreich). Systematik. Stratigraphie. Münchner geowissenschaftliche Abhandlungen. Reihe A, Geologie und Paläontologie 1, 1–161.
Marcucci, M., Kodra, A., Pirdeni, A., Gjata, T., 1994. Radiolarian assemblages in the Triassic and Jurassic cherts of Albania. Ofioliti 19 (1), 105–114.
Matsuoka, A., 2007. Living radiolarian feeding mechanisms: new light on past marine ecosystems. Swiss J Geosci 100, 273–279.
Meister, P., McKenzie, J.A., Bernasconi, S.M., Brack, P., 2013. Dolomite formation in the shallow seas of the Alpine Triassic. Sedimentology 60, 270–291.
Mrdak, M., Đaković, M., Gawlick, H.-J., Djerić, N., Bucur, I.I., Sudar, M., et al., 2024. Middle Triassic stepwise deepening and stratigraphic condensation associated with Illyrian volcanism in the Durmitor Mountain. Montenegro. Facies 70. doi:10.1007/s10347-024-00683-0, article no 10.
Mudrenović, V., Gaković, J., 1964. Prilog poznavanju razvoja srednjeg i gornjeg trijasa u dolini Zalomske Rijeke (Istočna Hercegovina). Geološki Glasnik Sarajevo 10, 139–157 Pls. 1-6.
Müller, J., 1858. Über die Thalassicollen, polycystinen und Acanthometren des Mittelmeeres. Abhandlungen der Königlichen Akademie der Wissenschaften zu Berlin, Jahre 1858, 1–62.
Nakaseko, K., Nishimura, A., 1979. Upper Triassic Radiolaria from southwest Japan. Sci Rep, Coll General Educ Osaka Univ 28, 61–109.
Obradović, J., Goričan, Š., 1988. Siliceous deposits in Yugoslavia: occurrences, types and ages. In: Hein, J.R., Obradović, J. (Eds.), Siliceous Deposits of the Tethys and Pacific Regions. Springer Verlag, pp. 51–64.
O'Dogherty, L., Carter, E.S., Dumitrica, P., Goričan, Š., De Wever, P., Hungerbühler, A., et al., 2009. Catalogue of Mesozoic radiolarian genera. Part 1: Triassic. Geodiversitas 31, 213–270.
O'Dogherty, L., Carter, E.S., Goričan, Š., Dumitrica, P.Lucas, S.G. (Ed.), 2010. Triassic radiolarian biostratigraphy. Triassic Timescale. Geol Soc London, Special Publ 334, 163–200.
Ogg, J.G., Ogg, G.M., Gradstein, F.M., 2016. A Concise Geologic Time Scale 2016. Elsevier, Amsterdam, p. 234.
Onodera, J., Takahashi, K., Jordan, R.W., 2008. Eocene silicoflagellate and ebridian paleoceanography in the central Arctic Ocean. Paleoceanography 23 PA1S15.
Orchard, M.J.Lucas, S. (Ed.), 2010. Triassic conodonts and their role in stage boundary definition. Triassic Timescale. Geol Soc London, Spec Publ 334, 139–161.
Ozsvárt, P., Kovács, S., 2012. Revised Middle and Late Triassic radiolarian ages for ophiolite mélanges: implications for the geodynamic evolution of the northern part of the early Mesozoic Neotethyan subbasins. Bulletin de la Société géologique de France 183 (4), 273–286.
Ozsvárt, P., Dosztály, L., Migiros, G., Tselepis, V., Kovács, S., 2012. New radiolarian biostratigraphic age constraints on Middle Triassic basalts and radiolarites from the Inner Hellenides (Northern Pindos and Othris Mountains, Northern Greece). Int J Earth Sci 101, 1487–1501.
Ozsvárt, P., Moix, P., Kozur, H.W., 2015. New Carnian (Upper Triassic) radiolarians from the Sorgun Ophiolitic Mélange, southern Turkey. Neues Jahrbuch für Geologie und Paläontologie Abhandlungen 277 (3), 337–352.
Ozsvárt, P., Dumitrica, P., Hungerbühler, A., Moix, P., 2017. Mono- and dicyrtid Nassellaria (Radiolaria) from the Upper Carnian of the Sorgun ophiolitic Mélange, Southern Turkey and Kopría Mélange, Rhodes, Greece. Revue de micropaléontologie 60, 137–160.
Ozsvárt, P., Rieber, H., Brack, P., 2023. Middle Triassic radiolarians from the Dolomites, Southern Alps, Italy. Geo.Alp 20, 5–100.
Parrish, J.T., 1993. Climate of the supercontinent Pangea. Journal of Geology 101, 215–233.
Pessagno, E.A., Six, W.M., Yang, Q., 1989. The Xiphostylidae Haeckel and Parvivaccidae, n. fam., (Radiolaria) from the North American Jurassic. Micropaleontology 35 (3), 193–255.
Peters, K.E., Cassa, M.R., 1994. Applied Source Rock Geochemistry. In: Magoon, L.B., Dow, W.G. (Eds.). In: The Petroleum System – From Source to Trap. The American Association of Petroleum Geologists Memoir 60, pp. 93–117.
Piros, O., Preto, N., 2008. Dasycladalean algae distribution in ammonoid-bearing Middle Triassic platforms (Dolomites, Italy). Facies 54, 581–595.
Pott, C., Kerp, H., Krings, M., 2008. Sphenophytes from the Carnian (Upper Triassic) of Lunz am See (Lower Austria). Jahrbuch der Geologischen Bundesanstalt 148 (2), 183–199.
Preto, N., Kustatscher, E., Wignall, P.B., 2010. Triassic climates – State of the art and perspectives. Palaeogeogr Palaeoclimatol Palaeoecol 290, 1–10.
Preto, N., Franceschi, M., Gattolin, G., Massironi, M., Riva, A., Gramigna, P., et al., 2011. The Latemar: a Middle Triassic polygonal fault-block platform controlled by synsedimentary tectonics. Sediment. Geol. 234, 1–18.
Ramovš, A., Goričan, Š., 1995. Late Anisian–Early Ladinian radiolarians and conodonts from Šmarna Gora near Ljubljana. Slovenia. Razprave IV. Razreda SAZU 36, 179–221.
Rampnoux, J.-P., 1974. Contribution à l'étude géologiqe des Dinarides: un secteur de la Serbie méridionale et du Monténégro oriental (Yougoslavie). Mémoires de la Société géologique de France 119, 99.
Sashida, K., Igo, H., 1992. Triassic radiolarians from a limestone exposed at Khao Chiak near Phatthalung, southern Thailand. Transact Proceed Palaeontol Soc Japan, New Series 168, 1296–1310.
Sashida, K., Kamata, Y., Adachi, S., Munasri, 1999. Middle Triassic radiolarians from West Timor, Indonesia. J Paleontol 73 (5), 765–786.
Sashida, K., Igo, H., Adachi, S., Ueno, K., Kajiwara, Y., Nakornsri, N., et al., 2000. Late Permian to Middle Triassic radiolarian faunas from northern Thailand. J Paleontol 74 (5), 789–811.
Schettino, A., Turco, E., 2011. Tectonic history of the western Tethys since the Late Triassic. GSA Bulletin 123 (1–2), 89–105.
Schmid, S.M., Fügenschuh, B., Kounov, A., Maţenco, L., Nievergelt, P., Oberhänsli, R., et al., 2020. Tectonic units of the Alpine collision zone between Eastern Alps and western Turkey. Gondwana Res 78, 308–374.
Schmoker, J.W., Halley, R.B., 1982. Carbonate porosity versus depth: a predictable relation for South Florida. Am Assoc Petroleum Geologists Bulletin 66 (12), 2561–2570.
Shi, L., Feng, Q., Shen, J., Ito, T., Chen, Z.-Q., 2016. Proliferation of shallow-water radiolarians coinciding with enhanced oceanic productivity in reducing conditions during the Middle Permian, South China: evidence from the Gufeng Formation of western Hubei Province. Palaeogeogr Palaeoclimatol Palaeoecol 444, 1–14.
Slovenec, D., Šegvić, B., Halamić, J., Goričan, Š., Zanoni, G., 2020. An ensialic volcanic arc along the northwestern edge of Palaeotethys – Insights from the Mid-Triassic volcano-sedimentary succession of Ivanščica Mt. (northwestern Croatia). Geol J 55, 4324–4351.
Smirčić, D., Kolar-Jurkovšek, T., Aljinović, D., Barudžija, U., Jurkovšek, B., Hrvatović, H., 2018. Stratigraphic definition and correlation of Middle Triassic volcaniclastic facies in the External Dinarides: Croatia and Bosnia and Herzegovina. J Earth Sci 29 (4), 864–878.
Smirčić, D., Aljinović, D., Barudžija, U., Kolar-Jurkovšek, T., 2020. Middle Triassic syntectonic sedimentation and volcanic influence in the central part of the External Dinarides, Croatia (Velebit Mts.). Geological Quater 64 (1), 220–239.
Smirčić, D., Vukovski, M., Slovenec, D., Kukoč, D., Šegvić, B., Horvat, M., et al., 2024. Facies architecture, geochemistry and petrogenesis of Middle Triassic volcaniclastic deposits of Mt. Ivanščica (NW Croatia): evidence of bimodal volcanism in the Alpine–Dinaridic transitional zone. Swiss Journal of Geosciences 117, 5.

Stach, E., Mackowsky, M.-Th., Teichmüller, M., Taylor, G.H., Chandra, D., Teichmüller, R., 1982. Coal Petrology. Gebrüder Borntraeger, Berlin-Stuttgart, p. 535.

Stefani, M., Furin, S., Gianolla, P., 2010. The changing climate framework and depositional dynamics of Triassic carbonate platforms from the Dolomites. Palaeogeogr Palaeoclimatol Palaeoecol 290, 43–57.

Stockar, R., Dumitrica, P., Baumgartner, P.O., 2012. Early Ladinian radiolarian fauna from the Monte San Giorgio (Southern Alps, Switzerland): systematics, biostratigraphy and paleo(bio)geographic implications. Rivista Italiana di Paleontologia e Stratigrafia 118 (3), 375–437.

Sudar, M.N., Gawlick, H.-J., Lein, R., Missoni, S., Kovács, S., Jovanović, D., 2013. Depositional environment, age and facies of the Middle Triassic Bulog and Rid formations in the Inner Dinarides (Zlatibor Mountain, SW Serbia): evidence for the Anisian break-up of the Neotethys Ocean. Neues Jahrbuch für Geologie und Paläontologie Abhandlungen 269 (3), 291–320.

Sudar, M.N., Gawlick, H.-J., Bucur, I.I., Jovanović, D., Missoni, S., Lein, R., 2023. From shallow-water carbonate ramp to hemipelagic deep-marine carbonate deposition: part 2. Sirogojno (Klisura quarry) – the reference section of the Middle to Late Anisian Bulog sedimentary succession in the Inner Dinarides (SW Serbia). Geološki anali Balkanskog poluostrva 84 (2), 41–70.

Sugiyama, K., 1992. Lower and Middle Triassic radiolarians from Mt. Kinkazan, Gifu Prefecture, Central Japan. Transact Proceed Palaeontol Soc Japan, new Series 167, 1180–1223.

Sugiyama, K., 1997. Triassic and Lower Jurassic radiolarian biostratigraphy in the siliceous claystone and bedded chert units of the southeastern Mino Terrane, Central Japan. Bullet Mizunami Fossil Museum 24, 79–193.

Swanberg, N.R., Bjørklund, K.R., 1986. The radiolarian fauna of western Norwegian fjords: Patterns of abundance in the plankton. Mar. Micropaleontol. 11, 231–241.

Swanberg, N.R., Bjørklund, K.R., 1987. Radiolaria in the plankton of some fjords in western and northern Norway: The distribution of species. Sarsi 72, 231–244.

Šćavničar, B., Šćavničar, S., Šušnjara, A., 1984. Vulkanogeno-sedimentni srednji trijas na području potoka Suvaje (Svilaja pl., Vanjski Dinaridi). Acta geologica 14 (2), 35–82, 1–13 Pls.

Taylor, G.H., Teichmüller, M., Davis, A., Diessel, C.F.K., Littke, R., Robert, P., 1998. Organic Petrology. Gebrüder Borntraeger, Berlin-Stuttgart, p. 704.

Takahashi, K., Onodera, J., Tanaka, S., 2015. Significance of radiolarians in the middle Eocene Arctic basin for determining the degree of the connection to the Atlantic Ocean. In: Proceedings of 14th INTERRAD, Antalya, Turkey, pp. 195–196 March 22–26, 2015.

Tekin, U.K., Sönmez, I., 2010. Late Ladinian radiolarians from the Tahtalidag Nappe of the Antalya nappes, SW Turkey: remarks on the late Middle and Late Triassic evolution of the Tahtalidag Nappe. Acta Geologica Polonica 60 (2), 199–217.

Velledits, F., 2006. Evolution of the Bükk Mountains (NE Hungary) during the Middle-Late Triassic asymmetric rifting of the Vardar-Meliata branch of the Neotethys Ocean. Int J Earth Sci (Geologische Rundschau) 95, 395–412.

Velledits, F., Péró, C., Bau, J., Senowbari-Daryan, B., Kovács, S., Piros, O., et al., 2011. The oldest Triassic platform margin reef from the Alpine-Carpathian region (Aggtelek, NE Hungary): Platform evolution, reefal biota and biostratigraphic framework. Rivista Italiana di Paleontologia e Stratigrafia 117 (2), 221–268.

Vishnevskaya, V.S., Djerić, N., Zakariadze, G.S., 2009. New data on Mesozoic Radiolaria of Serbia and Bosnia, and implications for the age and evolution of oceanic volcanic rocks in the Central and Northern Balkans. Lithos 108, 72–105.

Vlahović, I., Tišljar, J., Velić, I., Matičec, D., 2005. Evolution of the Adriatic Carbonate Platform: Palaeogeography, main events and depositional dynamics. Palaeogeogr Palaeoclimatol Palaeoecol 220, 333–360.

Yeh, K.-Y., 1990. Taxonomic studies of Triassic Radiolaria from Busuanga Island, Philippines. Bulletin Natl Museum Natur Sci 2, 1–63.

Zappaterra, E., 1994. Source-rock distribution model of the Periadriatic region. Am Assoc Petroleum Geologists Bulletin 78 (3), 333–354.